ESC European Society of Cardiology

Cardiovascular Research (2024) **120**, 301–317
https://doi.org/10.1093/cvr/cvae004

Hypertrophic cardiomyopathy dysfunction mimicked in human engineered heart tissue and improved by sodium–glucose cotransporter 2 inhibitors

Paul J.M. Wijnker [1,2]*, Rafeeh Dinani[1,2], Nico C. van der Laan[1,2], Sila Algül[1,2], Bjorn C. Knollmann[3], Arie O. Verkerk [2,4], Carol Ann Remme[2,4], Coert J. Zuurbier[2,5], Diederik W.D. Kuster[1,2], and Jolanda van der Velden [1,2]*

[1]Department of Physiology, Amsterdam UMC, Vrije Universiteit Amsterdam, De Boelelaan 1117, 1081 HV Amsterdam, The Netherlands; [2]Amsterdam Cardiovascular Sciences, Heart Failure & Arrhythmias, De Boelelaan 1108, 1081 HZ Amsterdam, The Netherlands; [3]Vanderbilt Center for Arrhythmia Research and Therapeutics, Division of Clinical Pharmacology, Vanderbilt University Medical Center, Nashville, TN, USA; [4]Experimental Cardiology, Amsterdam UMC, Academic Medical Centre, Amsterdam, The Netherlands; and [5]Laboratory for Experimental Intensive Care and Anesthesiology (L.E.I.C.A.), Department of Anesthesiology, Amsterdam UMC, Academic Medical Centre, Amsterdam, The Netherlands

Received 1 December 2022; revised 15 November 2023; accepted 29 November 2023; online publish-ahead-of-print 18 January 2024

Time of primary review: 35 days

Aims

Hypertrophic cardiomyopathy (HCM) is the most common inherited cardiomyopathy, often caused by pathogenic sarcomere mutations. Early characteristics of HCM are diastolic dysfunction and hypercontractility. Treatment to prevent mutation-induced cardiac dysfunction is lacking. Sodium–glucose cotransporter 2 inhibitors (SGLT2i) are a group of antidiabetic drugs that recently showed beneficial cardiovascular outcomes in patients with acquired forms of heart failure. We here studied if SGLT2i represent a potential therapy to correct cardiomyocyte dysfunction induced by an HCM sarcomere mutation.

Methods and results

Contractility was measured of human induced pluripotent stem cell-derived cardiomyocytes (hiPSC-CMs) harbouring an HCM mutation cultured in 2D and in 3D engineered heart tissue (EHT). Mutations in the gene encoding β-myosin heavy chain (*MYH7*-R403Q) or cardiac troponin T (*TNNT2*-R92Q) were investigated. In 2D, intracellular [Ca^{2+}], action potential and ion currents were determined. HCM mutations in hiPSC-CMs impaired relaxation or increased force, mimicking early features observed in human HCM. SGLT2i enhance the relaxation of hiPSC-CMs, to a larger extent in HCM compared to control hiPSC-CMs. Moreover, SGLT2i-effects on relaxation in R403Q EHT increased with culture duration, i.e. hiPSC-CMs maturation. Canagliflozin's effects on relaxation were more pronounced than empagliflozin and dapagliflozin. SGLT2i acutely altered Ca^{2+} handling in HCM hiPSC-CMs. Analyses of SGLT2i-mediated mechanisms that may underlie enhanced relaxation in mutant hiPSC-CMs excluded SGLT2, Na^+/H^+ exchanger, peak and late $Na_v1.5$ currents, and L-type Ca^{2+} current, but indicate an important role for the Na^+/Ca^{2+} exchanger. Indeed, electrophysiological measurements in mutant hiPSC-CM indicate that SGLT2i altered Na^+/Ca^{2+} exchange current.

Conclusion

SGLT2i (canagliflozin > dapagliflozin > empagliflozin) acutely enhance relaxation in human EHT, especially in HCM and upon prolonged culture. SGLT2i may represent a potential therapy to correct early cardiac dysfunction in HCM.

* Corresponding authors. E-mail: p.wijnker@amsterdamumc.nl (P.J.M.W.); E-mail: j.vandervelden1@amsterdamumc.nl (J.V.)

Graphical Abstract

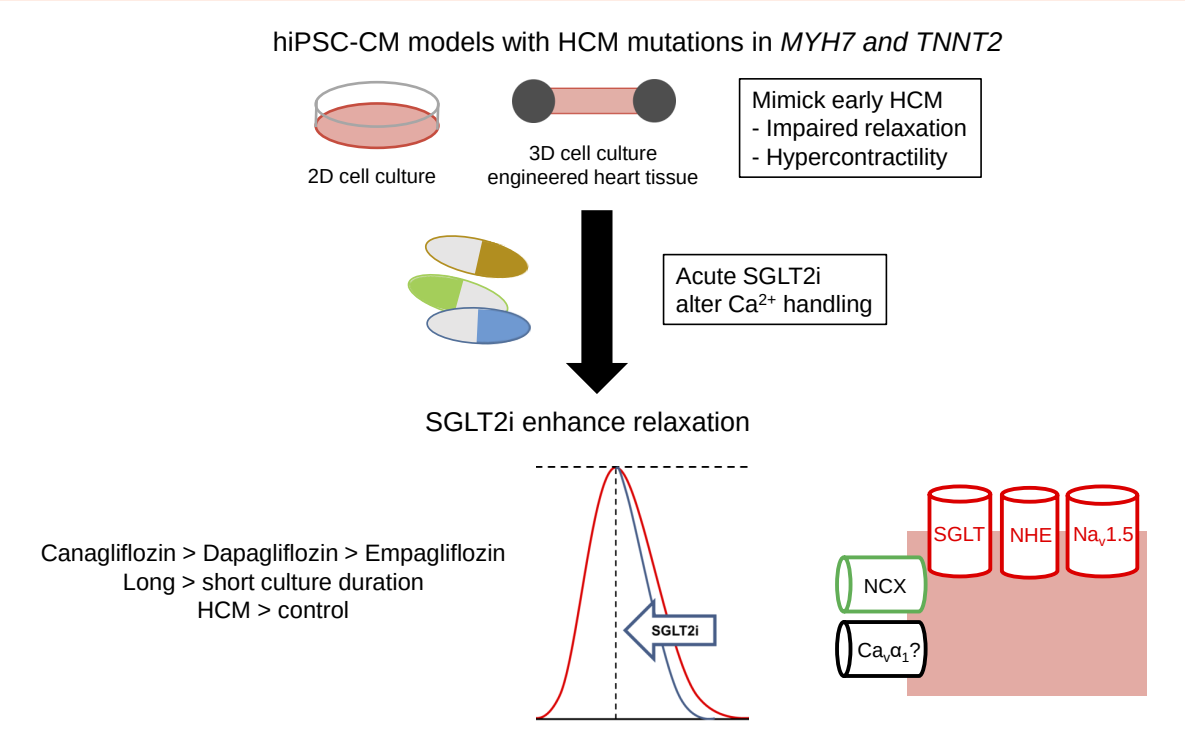

Keywords Hypertrophic cardiomyopathy • Sodium–glucose cotransporter 2 inhibitors • Human induced pluripotent stem cell-derived cardiomyocytes • Engineered heart tissue • Contractility • Ca^{2+} handling

1. Introduction

Hypertrophic cardiomyopathy (HCM) is the most common inherited cardiomyopathy, with an estimated prevalence of 1:500 to 1:200 in the general population.[1,2] The HCM clinical phenotype is characterized by asymmetric hypertrophy and diastolic dysfunction, with preserved or even slightly increased left ventricular ejection fraction. The most frequent cause of HCM are pathogenic gene variants, i.e. mutations, in genes encoding cardiac sarcomere proteins, the contractile building blocks of the heart. Among the most frequently affected genes in HCM are *MYH7* and *TNNT2*, encoding the thick-filament protein β-myosin heavy chain (β-MyHC) and the thin-filament protein cardiac troponin T (cTnT), respectively.[1,3] Despite increased knowledge of the pathomechanisms induced by HCM mutations, treatment to prevent or reverse disease is lacking.[4,5]

Sodium–glucose cotransporter 2 inhibitors (SGLT2i) are a group of antidiabetic drugs that promote urinary excretion of glucose and have been recently shown to have surprisingly large beneficial cardiovascular outcomes in patients with acquired forms of heart failure. The SGLT2i empagliflozin (Empa), canagliflozin (Cana), and dapagliflozin (Dapa) proved beneficial for diabetic and non-diabetic patients, acute and chronic heart failure patients, and for patients with heart failure with reduced ejection fraction (HFrEF) and preserved ejection fraction (HFpEF).[6–8] The reported beneficial cardiovascular effects are most likely the result of both on-target effects in the kidney (SGLT2 inhibition) and off-target effects in other organs.[9]

Multiple SGLT2i off-target effects have been reported in cardiomyocytes. SGLT2i directly inhibit two cardiac sodium transporters, the Na^+/H^+ exchanger (NHE-1) and $Na_v1.5$.[10–13] Inhibition of NHE-1 by Empa lowered cytosolic $[Na^+]$ and $[Ca^{2+}]$ in rabbit cardiomyocytes, whereas inhibition of $Na_v1.5$ reduced late Na^+ current ($I_{Na\text{-}Late}$) in cardiomyocytes from mice with heart failure or diabetic rats.[10,11,13] Empa also lowered cytosolic reactive oxygen species (ROS) in cardiomyocytes from diabetic rats and reduced oxidative stress in HFpEF.[13,14] Moreover, Dapa reduced the amplitude of L-type Ca^{2+} currents ($I_{Ca,L}$) and of shortening in cardiomyocytes from control (Ctrl) and diabetic rats.[15] Empa treatment also increased phosphorylation levels of cardiac troponin I (cTnI), cardiac myosin-binding protein-C (cMyBP-C), and phospholamban (PLB),[14,16,17] which may enhance cardiac muscle relaxation.[18,19] Finally, chronic treatment of HFpEF rats with a dual SGLT1&2 inhibitor (sotagliflozin) increased Na^+/Ca^{2+} exchanger (NCX) forward-mode activity on cytosolic Ca^{2+} removal in cardiomyocytes.[20] These potential cardiac targets of SGLT2i all have been implicated in HCM pathology.[4,21–25] Therefore, SGLT2i may represent a beneficial therapy in HCM.

To define if SGLT2i correct early cardiomyocyte dysfunction in HCM, we here investigated whether SGLT2i have direct beneficial effects on the functional characteristics of human cardiomyocytes harbouring a thick (*MYH7*-R403Q) or thin (*TNNT2*-R92Q) filament protein mutation. To this end, we first defined the contractile phenotype caused by HCM mutations in human induced pluripotent stem cell-derived cardiomyocytes (hiPSC-CMs) cultured in 3D engineered heart tissue (EHT) or in 2D. Subsequently, the effects of Empa, Cana, and Dapa on contractility were investigated in Ctrl and HCM hiPSC-CMs. We also investigated the effect of the culture duration on hiPSC-CM maturity and on SGLT2i-mediated effects on contractility. Finally, we investigated which of the proposed molecular mechanisms of SGLT2i were responsible for the observed changes in contractility of HCM hiPSC-CMs.

We show that HCM mutations in hiPSC-CMs impair relaxation or increase force, thereby mimicking the early cardiac features observed in HCM patients. SGLT2i enhance the relaxation of hiPSC-CMs to a larger extent in HCM compared to Ctrl hiPSC-CMs. The effects of Cana on relaxation are more pronounced than Empa and Dapa, and these effects depend on culture duration, i.e. EHT maturation. SGLT2i acutely alter Ca^{2+} handling in HCM hiPSC-CMs. In-depth analyses of potential mechanisms indicate that altered NCX activity underlies the acute SGLT2i-enhanced relaxation in mutant hiPSC-CMs. We provide data that support SGLT2i as a potential therapy to correct cardiac dysfunction in HCM.

2. Methods

2.1 Detailed methods descriptions are provided in Supplementary material online, methods section

2.1.1 Study approval, human EHT generation, treatment, and contraction measurements

Written informed consent was obtained from each patient in this study, and all procedures were performed according to the Declaration of Helsinki and were approved by the local medical ethics review committees.

The 3D EHT model promotes hiPSC-CMs maturation and allows a physiological way of contraction against auxotonic load.[26] Fibrin-based human EHTs were generated in agarose casting moulds with solid silicone racks as previously described, with small modifications.[27,28] EHTs were generated from hiPSC-CM harbouring an R403Q mutation in *MYH7* (R403Q; Fujifilm Cellular Dynamics, R1082), the isogenic control line of R403Q-*MYH7* (R403Qic; Fujifilm Cellular Dynamics, R1129), and unrelated healthy control cardiomyocytes (Ctrl; iCell Cardiomyocytes,[2] Fujifilm Cellular Dynamics, C1016).

Contractile analysis was performed in spontaneously beating and in electrically stimulated (2 V, 1 Hz, biphasic pulses of 4 ms) EHTs.[28] Investigating drug effects on contractility in spontaneously beating EHT allows us to measure chronotropic drug effects. In addition, the low beating rate of the EHT was an advantage, since it has been demonstrated that the accuracy in determining whether drugs will alter the contractility of the human heart, was improved by reducing spontaneous beat rate below 0.5 or 1 Hz by pharmacological blockage with ivabradine or selecting hiPSC-CMs with slow intrinsic beating rates.[29] Measurements in electrically stimulated EHT allowed direct comparison between different lines and verified if SGLT2i-effects were also observed at physiological beating rates. Measurements were performed at 15 min and 1 h before and after cumulative drug treatment. The contraction peaks were analysed in terms of frequency, force, and contraction time ($T1_{80\%}$) and relaxation time ($T2_{80\%}$) at 80% of peak height (*Figure 1A–C*).

2.1.2 2D hiPSC-CM culture, treatment and contraction, Ca^{2+} measurements, and cellular electrophysiology

R403Q-*MYH7*: R403Q and R403Qic were thawed, plated, and cultured on the Matrigel-coated µ-plate 24 well black (Ibidi, 82426) for 4 weeks according to manufacture instructions. Human iPSC-CMs were 58–60 days old at the time of the measurements.

R92Q-*TNNT2*: hiPSCs harbouring the R92Q mutation in *TNNT2* (R92Q-*TNNT2*) and the isogenic control line of R92Q-*TNNT2* (R92Qic) were thawed and cultured on Matrigel-coated plates. When cells reached 80–90% confluency the hiPSC cells were differentiated into hiPSC-CMs utilizing a chemically defined cardiomyocyte differentiation protocol.[30] 2D Contractility and Ca^{2+} measurements were performed 60 days post differentiation.

Simultaneous measurements of contractility and Ca^{2+} kinetics were performed on the monolayer of spontaneously beating iPSC-CMs, using the CytoCypher MultiCell High Throughput System as recently described.[31] For each well, measurements were performed 15 min before and after SGLT2i treatment. Single-cell patch clamp studies were performed in R92Q-*TNNT2* to define the effect of SGLT2i on cellular electrophysiology.

2.2 Protein extraction and western blot analysis

EHTs were processed by mechanical tissue lysing as described before.[28] Proteins were separated on precast SDS–PAGE 4–12% criterion gels (Bio-Rad) and electrotransferred to polyvinylidene difluoride membranes.

2.3 L-type Ca^{2+} channel binding assays

Cana binding (five concentrations, two replicates) to the diltiazem site, verapamil site, and the dihydropyridine site of the L-type Ca^{2+} channel was investigated by Eurofins, and the IC_{50} was calculated. Results are expressed as percent inhibition of the control radioligand-specific binding.

2.4 L-type Ca^{2+} channel patch clamp assay

An electrophysiological Cav1.2 human Ca^{2+} ion channel cell-based QPatch CiPA assay was conducted by Eurofins (Eurofins, CYL8051QP2DR) to profile Empa, Cana, and Dapa (five compound concentrations and two replicates) for activities on the L-type Ca^{2+} channel using the QPatch electrophysiological platform, and IC_{50} values were calculated.

2.5 Patch clamp experiments hiPSC-CM

Patch clamp studies were performed in R92Q-*TNNT2* hiPSC-CMs to test the effects of Cana on action potentials (APs), peak and late I_{Na}, NCX current (I_{NCX}), and $I_{Ca,L}$.

2.6 Statistical analysis

Data are presented as mean ± standard error of the mean (SEM) in bar graphs and as single values in scatterplots. Statistical analyses were performed by (repeated) one-way ANOVA followed by Dunnett's or Tukey's post-test or by (un)paired Student's *t*-test as indicated, using the software GraphPad Prism8. If EHTs stopped beating as a result of drug treatment, a mixed-effects analysis followed by Dunnett's post-test was performed. A value of $P < 0.05$ was considered statistically significant.

3. Results

3.1 Empa enhances relaxation and effects are larger in HCM compared to control EHT

We examined acute Empa effects in spontaneously beating EHT. Clinically relevant (1 µM) and high (10, 50 µM) Empa concentrations were tested to investigate toxicity and dose-response effects. Empa treatment significantly reduced force, relaxation time, and contraction velocity in a dose-dependent manner in R403Q, R403Qic, and unrelated healthy control (Ctrl) EHTs (*Figure 1D* and *E* and Supplementary material online, *Figure S1A* and *B*). Noteworthy, Empa only exerted significant effects at 1 µM in R403Q (*Figure 1E* and Supplementary material online, *Figure S1A*), and Empa effects on relaxation were significantly larger in R403Q compared to R403Qic (*Figure 1F*). No chronotropic Empa effects (see Supplementary material online, *Figure S1A* and *B*) or DMSO effects on contractility (see Supplementary material online, *Figure S2*; vehicle control) were observed.

The HCM phenotype and Empa effects were also examined in electrically stimulated EHT (1 Hz), which allows comparisons at the same beating rate (*Figure 2A*). The width of the R403Q and R403Qic EHTs did not differ (*Figure 2B*; EHT images in Supplementary material online, *Figures S3* and *S4*). Force was significantly higher in R403Q compared to R403Qic (*Figure 2B*), in line with the cardiac HCM phenotype. In addition, contraction velocity and relaxation velocity were significantly higher in paced R403Q compared to R403Qic, while relaxation time did not differ (*Figure 2B* and Supplementary material online, *Figure S5A*). Empa reduced force, relaxation time, and contraction velocity in a dose-dependent manner in R403Q, R403Qic, and control EHTs (*Figure 2C* and *D* and Supplementary

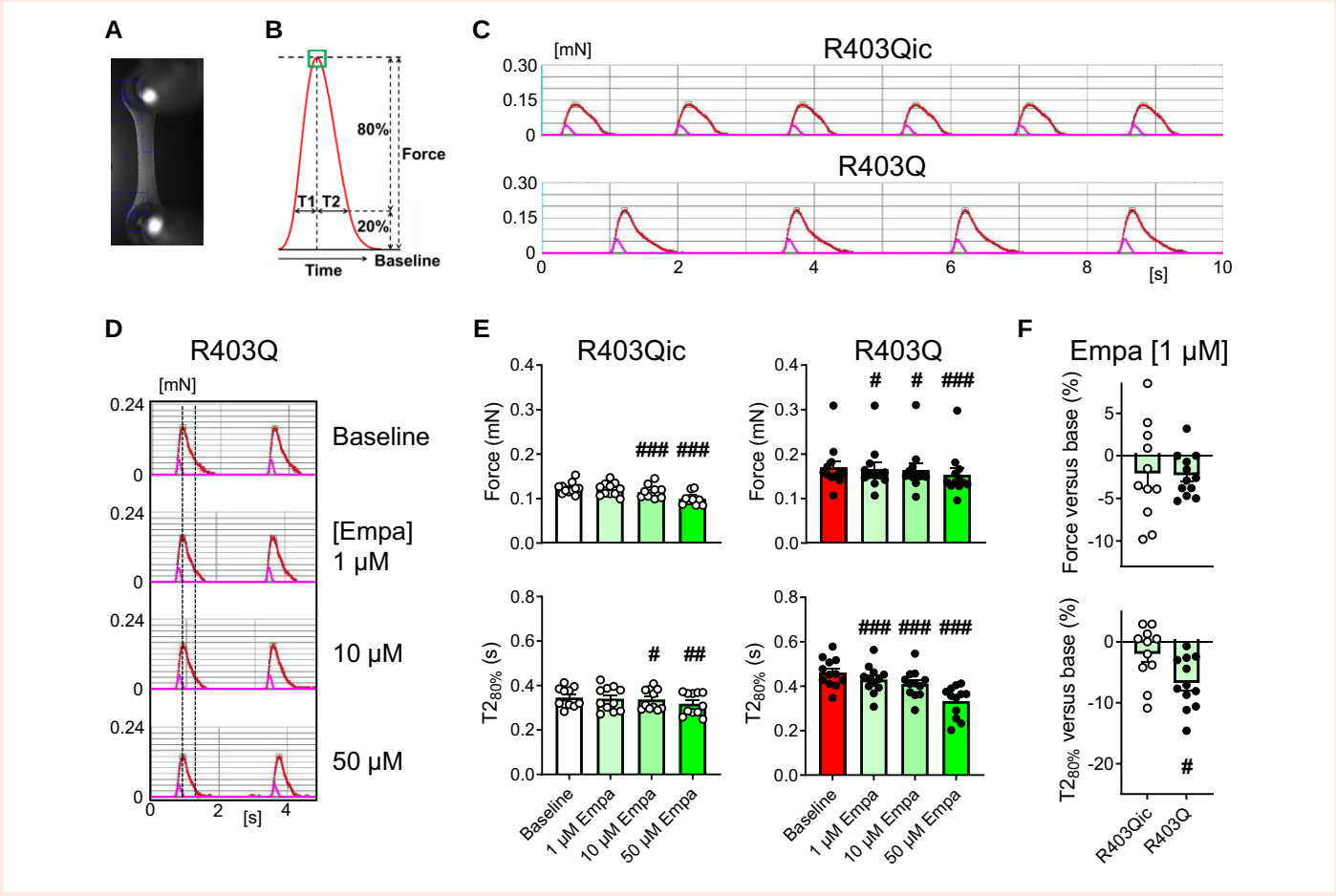

Figure 1 Contractile phenotype and Empa treatment of spontaneously beating R403Q EHTs. (*A*) Representative picture of a human EHT as viewed by the video camera and evaluated by automated figure recognition (squares). (*B*) Schematic contraction peak with evaluated parameters of contractile function. (*C*) Examples of spontaneous beating patterns of R403Qic and R403Q EHT after 6 weeks of culture (red line, original recording; pink line, velocity). (*D*) Example of beating patterns of an R403Q EHT at baseline and after Empa treatment. Dotted lines allow us to compare the Empa effect on relaxation to baseline. (*E*) Effect of cumulative treatment with Empa for 1 h on contractility in starvation medium in R403Qic ($n = 11$, 39 ± 1 days) and R403Q ($n = 12$, 46 ± 3 days). (*F*) Comparison of the Empa (1 µM) effect between R403Qic and R403Q, calculated as the change in force or $T2_{80\%}$ as a percentage compared to baseline. Data are expressed as mean ± SEM (*E*, *F*; 2–3 independent EHT preparations). #$P < 0.05$, ##$P < 0.01$, ###$P < 0.001$ vs. Baseline (*E*) or R403Qic (*F*), repeated measures one-way ANOVA followed by Dunnett's post-test (E) or unpaired Student's *t*-test (*F*).

material online, *Figure S5B and C*). Empa effects on relaxation were significantly larger in R403Q compared to R403Qic (*Figure 2E*). No DMSO effects on contractility were observed in paced EHTs (see Supplementary material online, *Figure S6*; vehicle control). Overall, the data in spontaneously beating and paced EHT indicate that Empa predominantly enhances relaxation and effects are larger in HCM compared to control EHT.

3.2 Comparison of Empa, Cana, and Dapa effects on contractility in EHT

We also investigated if the Empa effects on contractility represent SGLT2i class effects. Cana (*Figure 3A* and Supplementary material online, *Figure S7A*) and Dapa (*Figure 3B* and Supplementary material online, *Figure S7B*) also lowered force, relaxation time, and contraction velocity in a dose-dependent manner in spontaneously beating R403Q, without chronotropic effects. Likewise, Cana (see Supplementary material online, *Figure S7C and E*) and Dapa (see Supplementary material online, *Figure S7D*) reduced relaxation time and contraction velocity in paced R403Q EHTs. Noteworthy, some EHTs stopped beating (*Figure 3A, B* and Supplementary material online, *Figure S7*) at high [(Cana) 10, 50 µM] or [(Dapa) 50 µM] and these EHTs completely recovered after washing out the SGLT2i. Interestingly, the Cana-mediated reduction in relaxation time in R403Q was significantly larger compared to Empa, with an intermediate effect of Dapa (*Figure 3C*). Cana (1 µM) also lowered relaxation time in R403Qic EHTs (see Supplementary material online, *Figure S8A*) with larger effects compared to Empa (see Supplementary material online, *Figure S8B*; $P = 0.06$). Like Empa, Cana effects were larger in R403Q than in R403Qic (*Figure 3D*). Overall, the SGLT2i-enhanced relaxation in EHT turns out to be a class effect, with Cana as the most effective SGLT2i.

3.3 SGLT2i-enhanced relaxation in R403Q EHT depends on culture duration

Prolonged R403Q culturing increased hiPSC-CMs maturity, evident from a large increase in the adult isoform cTnI during the first 70 days, and a coincident reduction of slow skeletal TnI (ssTnI) which is expressed in foetal myocardium (*Figure 4A*). We therefore treated EHTs multiple times for 1 h with SGLT2i on different days after EHT casting to investigate the effect of the culture duration. Strikingly, the acute SGLT2i-enhanced relaxation in

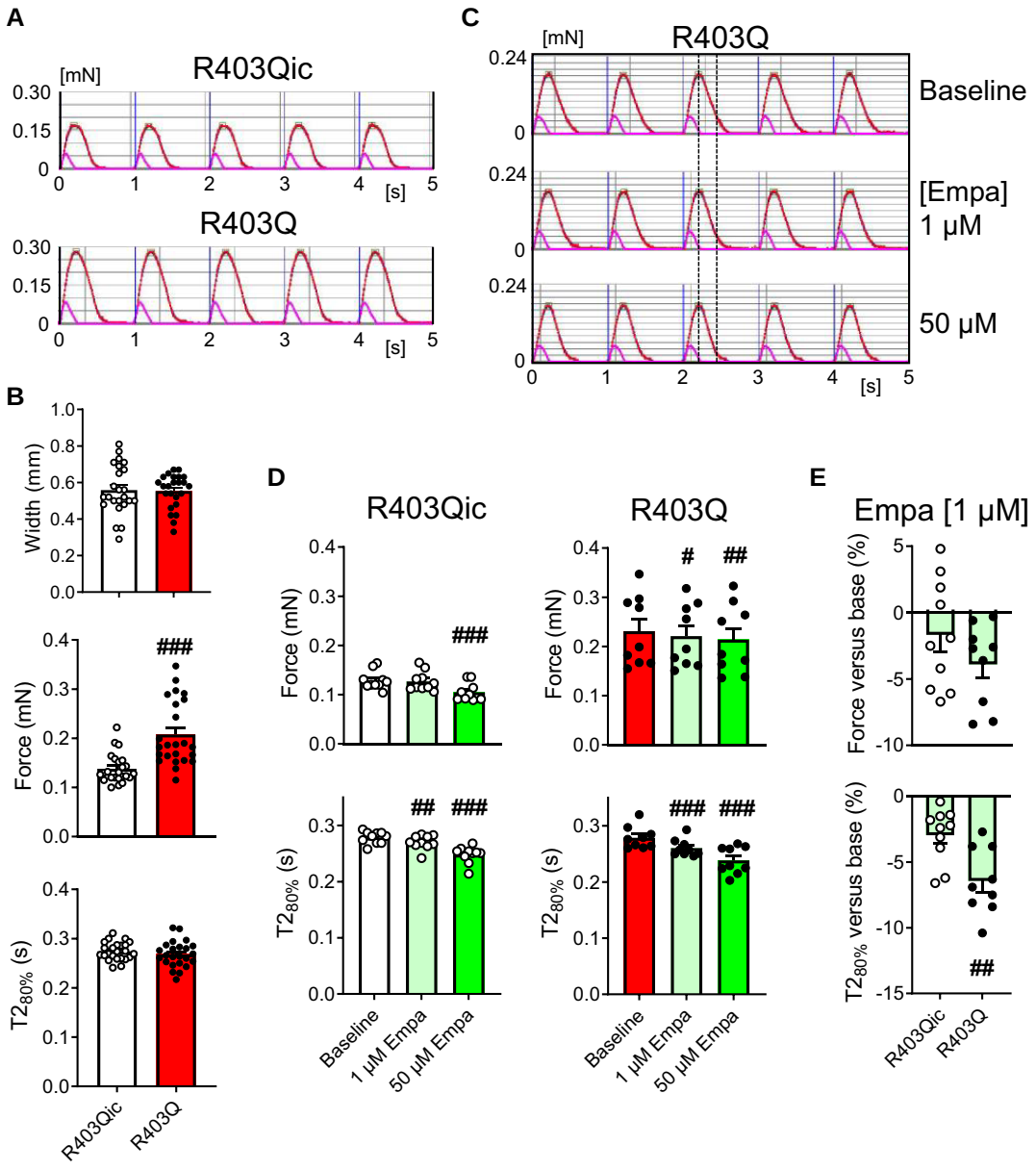

Figure 2 Contractile phenotype and Empa treatment of electrically stimulated R403Q EHTs. (*A*) Examples of beating patterns of an electrically stimulated (1 Hz) R403Qic and R403Q EHT (red line, original recording; pink line, and velocity). (*B*) EHT width, force of contraction and $T2_{80\%}$ of R403Qic ($n = 24$, 42 ± 3 days) were compared to R403Q ($n = 24$, 42 ± 0.2) EHTs paced at 1 Hz in starvation medium. (*C*) Example of beating patterns of an electrically stimulated (1 Hz) R403Q EHT at baseline and after Empa treatment. Dotted lines allow us to compare the Empa effect on relaxation to baseline. (*D*) Effect of Empa treatment for 1 h on contractility in starvation medium in R403Qic ($n = 10$, 39 ± 3 days) and R403Q ($n = 9$, 43 ± 0.2 days) paced at 1 Hz. (*E*) Comparison of the Empa (1 µM) effect on contractility between R403Qic and R403Q, calculated as the change compared to baseline. Data are expressed as mean ± SEM (*B*; three independent EHT preparations, *D*, *E*; two independent EHT preparations). $\#P < 0.05$, $\#\#P < 0.01$, $\#\#\#P < 0.001$ vs. R403Qic (*B*, *E*) or Baseline (*D*), unpaired Student's *t*-test (*B*, *E*) or Repeated measures one-way ANOVA followed by Dunnett's post-test (*D*).

R403Q strongly increased with culture time from day 20 until day 69 for all SGLT2i (*Figure 4B* and Supplementary material online, *Figure S9A*). Again, the effect size was SGLT2i-dependent (Cana > Dapa > Empa; *Figure 4C*). SGLT2i-effects were independent of the relaxation time at baseline, as this was stable from day 20 until day 55 (*Figure 4B*). Likewise, beating frequency did not differ between days 37 and 69 and stabilized from day 44 (*Figure 4B*). Moreover, also in paced (60 BPM) R403Qic EHT (*Figure 4D* and Supplementary material online, *Figure S9B*), the Empa-enhanced relaxation depended on culture duration. SGLT2i-effects were independent of hypertrophy from day 20 until day 43 of EHT culture, since no significant differences in the hypertrophic markers [phosphorylated extracellular signal-regulated kinase (pERK)/ERK] and pAkt/Akt) were identified when comparing 42 or 43 days cultured R403Qic to R403Q and Ctrl EHT (see Supplementary material online, *Figure S9C*). After 91 days of culture of R403Q EHT, the ratios of pERK/ERK and pAkt/Akt were significantly increased compared to R403Q EHT at 43 days of culture (see Supplementary material online, *Figure S9C*). No increase in hypertrophic markers was observed in 97 days of cultured Ctrl EHT compared to 42

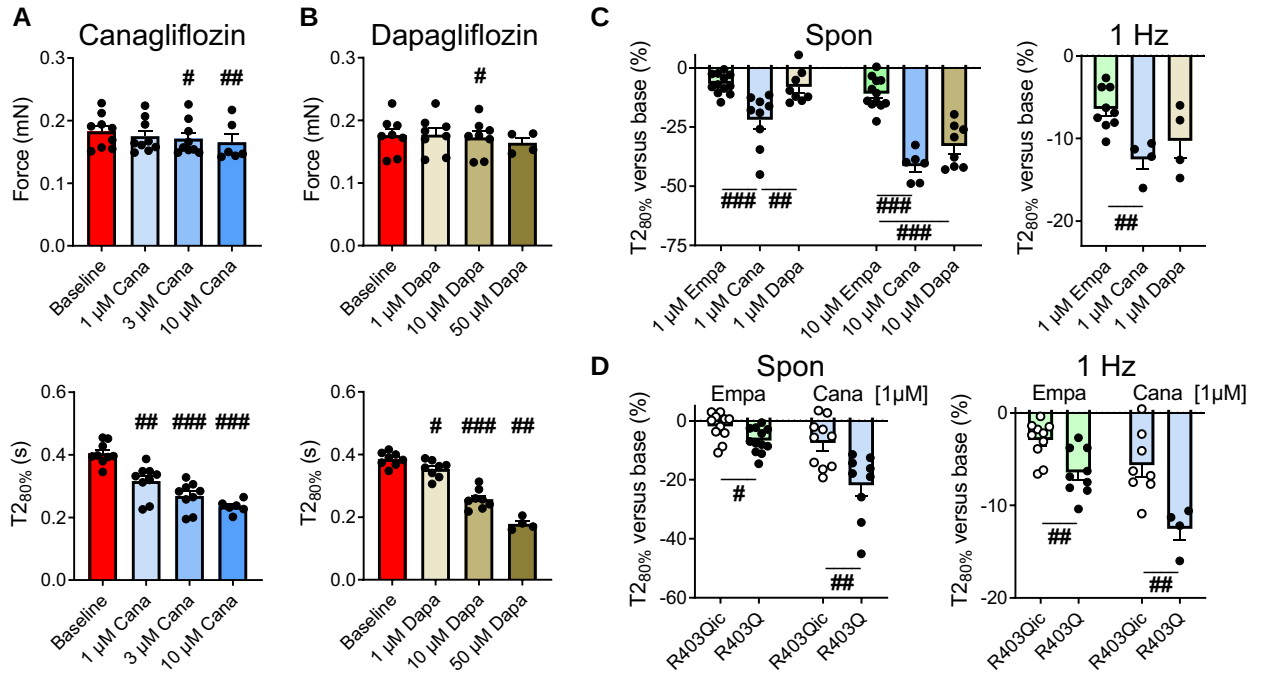

Figure 3 Comparison of SGLT2i-effects on contractility in EHT. (*A*) Effect of Cana treatment for 1 h on force and $T2_{80\%}$ in spontaneously beating R403Q ($n = 9$, 52 ± 5 days). At 10 µM Cana, 3 EHTs stopped beating. (*B*) Effect of Dapa treatment for 1 h in spontaneously beating R403Q ($n = 8$, 48 ± 5 days). At 50 µM Dapa, 4 EHTs stopped beating. (*C*) Empa, Cana, and Dapa effects on $T2_{80\%}$ in spontaneously beating (Spon) and in paced (1 Hz) R403Q were compared to each other, calculated as the change in $T2_{80\%}$ as a percentage compared to baseline (Empa data from *Figures 1F* and *2E*). (*D*) The effect size on relaxation time of Empa and Cana was compared between R403Qic and R403Q, showing a significantly larger reduction in relaxation time upon Empa and Cana treatment in R403Q compared to R403Qic (Empa data from *Figures 1F* and *2E*, Cana data in R403Qic from Supplementary material online, *Figure S8B*). Data are expressed as mean ± SEM (*A*: two independent EHT preparations, *B*: one EHT preparation). (*A*, *B*) #$P < 0.05$, ##$P < 0.01$, ###$P < 0.001$ vs. Baseline or (*D*) R403Qic, (*A*, *B*) a mixed-effects analysis followed by Dunnett's post-test was performed if values are missing because EHTs stopped beating as a result of the treatment, or (*C*) one-way ANOVA followed by Tukey's multiple comparisons test, or (*D*) unpaired Student's *t*-test.

days of cultured Ctrl EHT (see Supplementary material online, *Figure S9D*). Overall, we show that SGLT2i-effects on relaxation strongly depend on the culture duration, i.e. EHT maturation.

3.4 Acute SGLT2i-effects on Ca^{2+} handling in 2D hiPSC-CM

Acute SGLT2i-effects on Ca^{2+} handling were investigated simultaneously with contraction kinetics in 2D hiPSC-CM after 28 days of culturing. In line with the R403Q EHT data at day 28 (*Figure 4B*), 1 µM Empa did not affect relaxation in 2D R403Q hiPSC-CM (*Figure 5A*), whereas a reduction in relaxation and Ca^{2+} decay time was detected at 10 µM Empa (*Figure 5A*, $P = 0.06$). No Empa effects (1 and 10 µM) on relaxation or Ca^{2+} handling were observed in 2D R403Qic (*Figure 5A* and Supplementary material online, *Figure S10A*). Cana at 1µM already lowered relaxation time in 2D R403Q (*Figure 5B*), as was observed on day 28 in EHTs (*Figure 4B*). Cana also lowered the Ca^{2+} decay time and the amplitude of the Ca^{2+} transient in R403Q (*Figure 5B*). To investigate if SGLT2i-effects are specific to the *MYH7*-R403Q mutation, we also tested Cana in *TNNT2*-R92Q hiPSC-CM. R92Q displayed a higher relaxation time and Ca^{2+} decay time compared to R92Qic, without differences in beating frequency (*Figure 5C* and Supplementary material online, *Figure S10C*). In R92Q, Cana reduced relaxation time ($P = 0.08$) and significantly reduced the amplitude of the Ca^{2+} transient (*Figure 5D*). Overall, SGLT2i treatment acutely affected Ca^{2+} handling in HCM hiPSC-CMs, with larger Cana effects compared to Empa.

3.5 Molecular targets of SGLT2i-enhanced relaxation in R403Q EHT

The next step was to investigate which of the SGLT2i-targets mediate the SGLT2i-enhanced R403Q relaxation. To this end, drug effects (cariporide, ranolazine, SS-31, diltiazem, SEA0400, and YM-244769) were investigated in slowly beating EHT, since SGLT2i also improved relaxation in slowly beating EHT and since the slow beating rate of EHT has been demonstrated to improve the accuracy in determining whether drugs will alter contractility of human stem cell-derived heart preparations.[29]

SGLT2: In glucose and insulin-free conditions, Empa (0.5–50 µM, 1 h) also reduced relaxation time and force (*Figure 6A* and Supplementary material online, *Figure S11A*). In addition, SGLT2 expression was not detected via western blot in EHT (see Supplementary material online, *Figure S12A*). This suggests that the Empa effects on relaxation are independent of SGLT2 activity.

NHE-1: NHE-1 was expressed in R403Q and did not differ from R403Qic (see Supplementary material online, *Figure S12A*). The selective NHE-1 inhibitor cariporide (*Figure 6B* and Supplementary material online, *Figure S11B*) did not reduce force and relaxation time at 1 and 10 µM (*Figure 6B*) in R403Q, while a relatively small reduction in relaxation time was observed at 50 µM. At 250 µM cariporide, three of nine EHTs stopped beating (data not shown).

$Na_v1.5$: $Na_v1.5$ was expressed in EHT (see Supplementary material online, *Figure S12B*). The $Na_v1.5$ antagonist and $I_{Na\text{-}Late}$ inhibitor ranolazine hydrochloride (*Figure 6C* and Supplementary material online, *Figure S11C*)

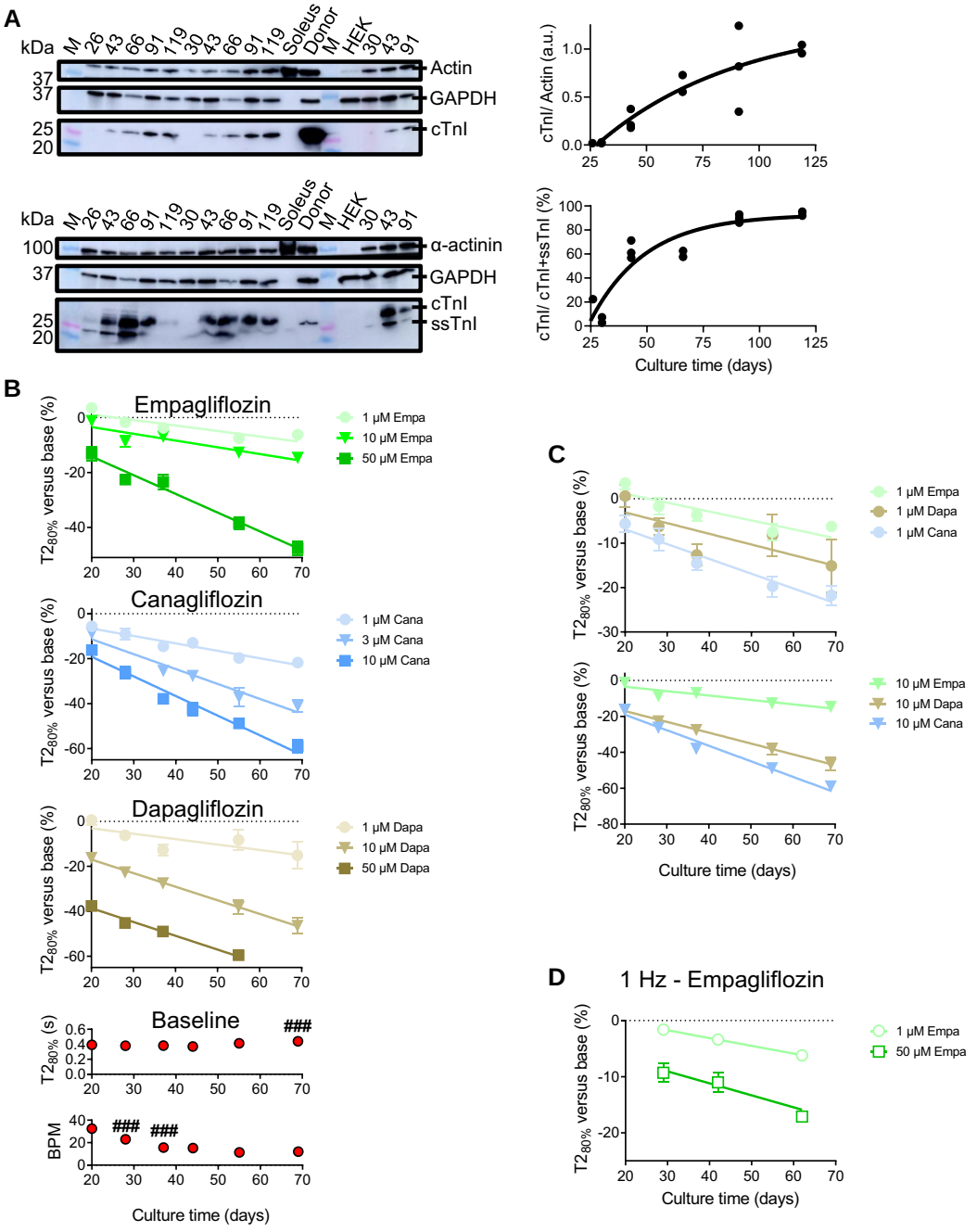

Figure 4 SGLT2i-effect on relaxation time in R403Q EHT depends on culture duration. (*A*) Western blots of R403Q EHTs stored on different days after EHT casting, as indicated above each lane. A human donor sample (donor) was loaded as a positive control for cardiac troponin I (cTnI), a mouse soleus sample as a positive control for slow skeletal troponin I (ssTnI), and HEK 293 cells as a negative control for TnI. cTnI expression corrected for actin increased upon prolonged culture time of R403Q EHT. This was also demonstrated with an antibody that detects both cTnI and ssTnI. Glyceraldehyde-3-phosphate dehydrogenase (GAPDH) and α-actinin staining illustrate that similar amounts of protein were loaded in each lane. The cTnI blot was cut at ~50 kDa and ~100 kDa, and the cTnI-ssTnI blot was cut at ~85 kDa and ~43 kDa. (*B*) Spontaneously beating R403Q were treated with SGLT2i ($n = 3$–4 EHTs per SGLT2i) on different days after EHT casting with cumulative concentrations for 1 h. Measurements with Empa, Cana, and Dapa were performed on days 20, 28, 37, 55, and 69, and with Cana also on day 44. The effect of SGLT2i on $T2_{80\%}$ was expressed as SGLT2i-induced changes compared to the baseline expressed in percentage. At 10 µM Cana, 2 EHTs stopped beating at days 44, 55, and 69. At 50 µM Dapa, 1 EHT stopped beating on day 28, two EHTs on day 55, and all four EHTs on day 69. Baseline values of $T2_{80\%}$ before SGLT2i treatment were stable over time and were only significantly higher at day 69 compared to day 20 ($n = 12$ EHTs on days 20, 28, 37, and 55; $n = 4$ EHTs on day 44; and $n = 11$ EHTs on day 69). Baseline values of beating frequency (beats per minute, BPM) before SGLT2i treatment stabilized from day 44. (*C*) Empa, Cana, and Dapa effects on relaxation time in R403Q EHTs were also plotted together at the same concentration for a direct comparison between SGLT2i (data were plotted on the days when all three SGLT2i were tested). (*D*) The effect of Empa on $T2_{80\%}$ plotted against the culture duration of electrically stimulated (1 Hz) R403Qic EHTs ($n = 4$ on day 29, $n = 5$ on day 42, and $n = 1$ on day 62—data of *Figure 2*). Data are expressed as mean ± SEM (*B*, *C*: one EHT preparation, *D*: two independent EHT preparations). ###$P < 0.001$ vs. day 20, one-way ANOVA followed by Dunnett's post-test (*B*, Baseline $T2_{80\%}$), or one-way ANOVA followed by Tukey's multiple comparisons test (*B*, BPM). Linear regression lines (*B*–*D*) and non-linear lines (*A*, one phase decay) were fitted.

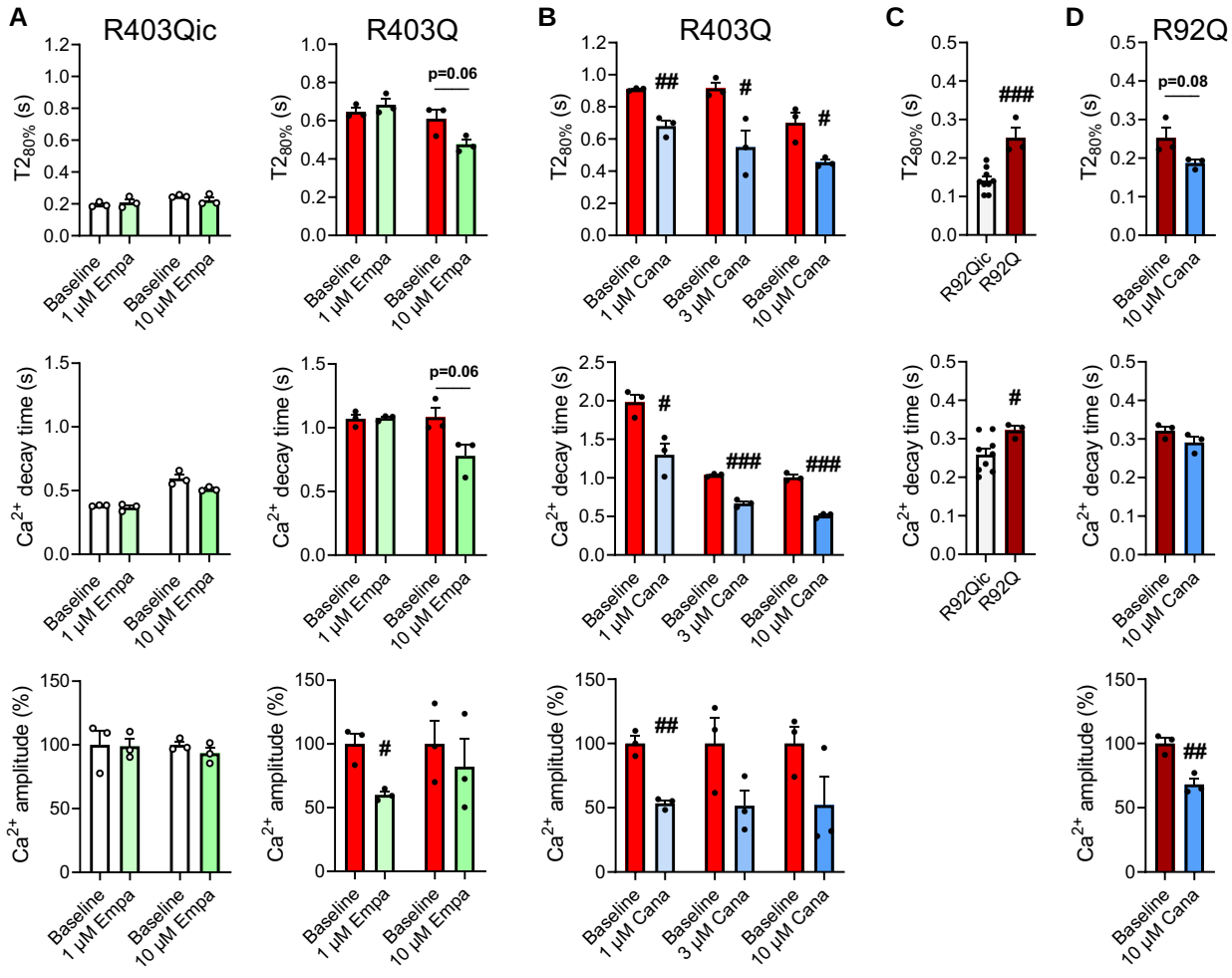

Figure 5 Empa and Cana effects on Ca^{2+} handling and contractility in 2D *MYH7*-R403Q and *TNNT2*-R92Q hiPSC-CM. R403Qic and R403Q (~30–32 days old) hiPSC-CM were thawed and cultured in 2D and after 4 weeks contraction kinetics and Ca^{2+} handling were measured simultaneously in Tyrode medium. Relaxation time ($T2_{80\%}$), Ca^{2+} transient decay time (Ca^{2+} decay time), and Ca^{2+} transient amplitude (Ca^{2+} amplitude) were measured. (*A*) R403Qic and R403Q hiPSC-CM treated for 15 min with 1 or 10 µM Empa. (*B*) R403Q hiPSC-CM treated for 15 min with 1, 3, or 10 µM Cana. (*C*) Contractile parameters of isogenic control hiPSC-CM (R92Qic) were compared to hiPSC-CM harbouring a *TNNT2*-R92Q mutation (R92Q) 35–45 days after thawing (60 days old). (*D*) R92Q were treated for 15 min with 10 µM Cana. The Ca^{2+} amplitude could only be determined as a relative change compared to the baseline. Each data point represents the average value of at least three spots measured within one well. Data are expressed as mean ± SEM. #$P < 0.05$, ##$P < 0.01$, ###$P < 0.001$ vs. (*A*, *B*, *D*) Baseline or (*C*) R92Qic, and (*A–D*) unpaired Student's *t*-test.

did not significantly lower relaxation time in R403Q. At 20 µM ranolazine, four of six EHTs stopped beating, and at 50 µM, all EHTs stopped beating.

ROS/NO: The mitochondrial antioxidant SS-31 (elamipretide, *Figure 6D* and Supplementary material online, *Figure S13A*) and the antioxidant N-acetylcysteine (NAC; Supplementary material online, *Figure S13B*) did not affect relaxation time in R403Q. To investigate the role of nitric oxide (NO), R403Q was pre-treated with 100 µM N(ω)-nitro-L-arginine methyl ester (L-NAME, 1 h) to inhibit NO production, followed by treatment with L-Name and Empa. Both in the absence and the presence of L-Name, Empa-enhanced relaxation (see Supplementary material online, *Figure S13C*).

PLB/cTnI/cMyBP-C phosphorylation: Empa (1, 50 µM) treatment of R403Q did not affect PLB mono-phosphorylation at Ser16 or Thr17 or bis-phosphorylation at Ser16/Thr17 (*Figure 6E, F* and Supplementary material online, *Figure S14A*). PLB-Ser16 mono-phosphorylation (*Figure 6E*) and PLB-Ser16/Thr17 bis-phosphorylation (see Supplementary material online, *Figure S14A*) were almost absent in untreated R403Q EHTs and were detected in the positive controls (donor heart, Ctrl EHT treated with isoprenaline). No Empa-mediated changes in cMyBP-C phosphorylation at Ser282 in R403Q were observed (*Figure 6E*). In addition, no phosphorylation of cTnI-Ser23/24 was detected in EHT (see Supplementary material online, *Figure S12C*; R403Q, R403Qic, Ctrl) and in Empa-treated R403Q (see Supplementary material online, *Figure S14B*).

L-type Ca^{2+} channel: EHT expressed the L-type Ca^{2+} channel ($Ca_v\beta_2$ subunit; Supplementary material online, *Figure S12D*). Contractile responses to the L-type Ca^{2+} channel blocker diltiazem were strikingly similar to SGLT2i in several aspects: (i) diltiazem and SGLT2i reduced force and relaxation time in R403Q and Ctrl (*Figure 7A* and Supplementary material online, *Figure S15*); (ii) higher concentrations of diltiazem and SGLT2i were needed to affect contractility in Ctrl compared to R403Q (100 nM in R403Q, 3 µM in Ctrl); (iii) diltiazem (*Figure 7A*) and SGLT2i (*Figures 1E* and *3A, B*) effects were more pronounced on relaxation compared to force in R403Q, whereas force was more affected compared to relaxation in Ctrl (*Figure 7A* and Supplementary material online, *Figure S1B*). Because of these similarities and a previous study showing that Dapa reduced the $I_{Ca,L}$,[15] we investigated via radioligand binding assays whether

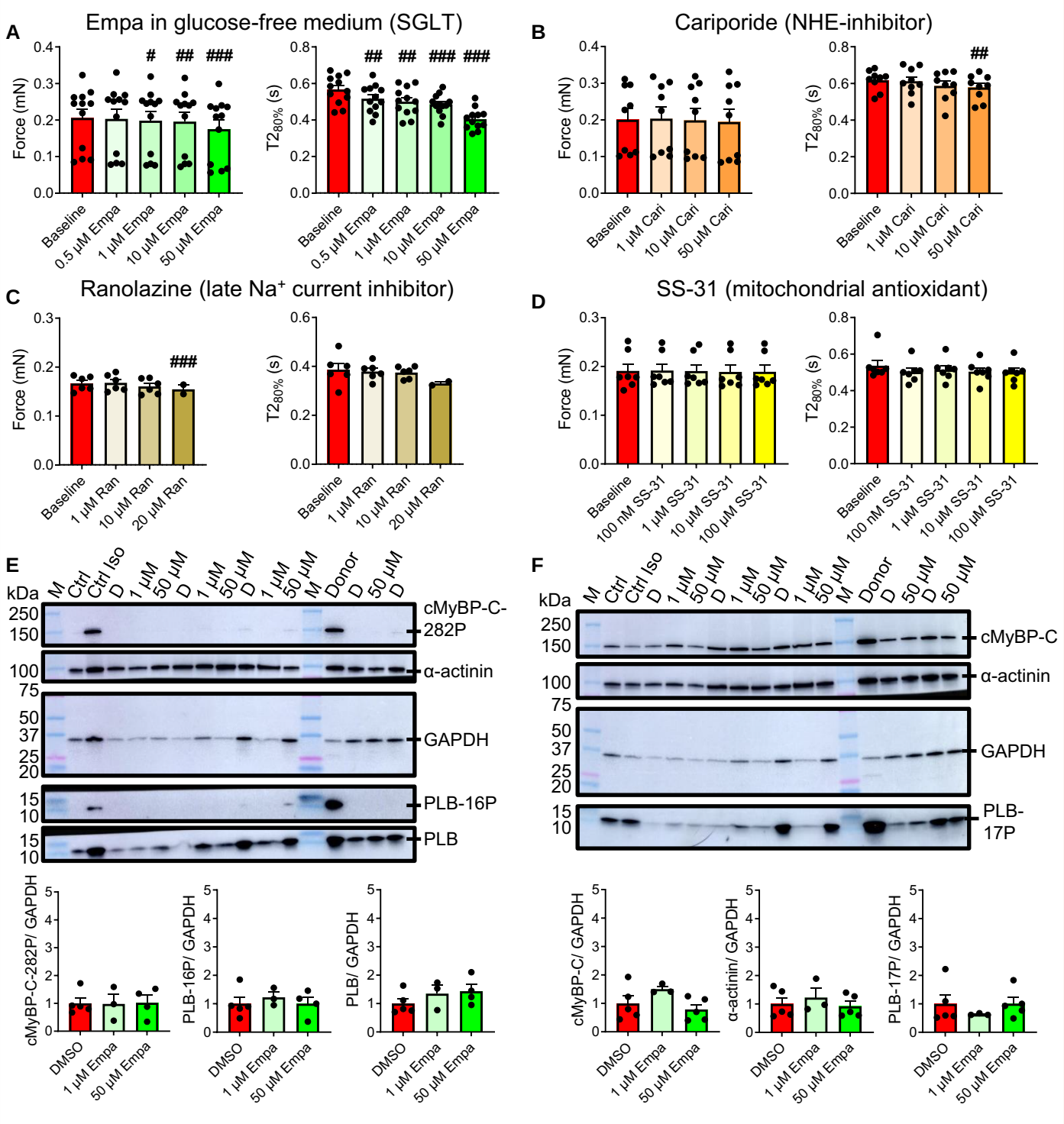

Figure 6 Potential molecular targets of SGLT2i investigated in R403Q EHT. (*A*) Empa treatment for 1 h lowers relaxation time of spontaneously beating R403Q ($n = 12$, 70 ± 10 days) in starvation medium without glucose and insulin. (*B*) Effect of treatment with the selective NHE-1 inhibitor cariporide (Cari) for 1 h on contractility in R403Q ($n = 9$, 61 ± 7 days). (*C*) Treatment with the late Na^+ current inhibitor ranolazine hydrochloride (Ran) for 1 h in spontaneously beating R403Q (1–50 µM: $n = 6$, 54 ± 6 days). (*D*) Effect of treatment with the mitochondrial antioxidant elamipretide (SS-31; $n = 7$, 79 ± 0 days) for 1 h on contractility in R403Q. (*E*, *F*) Western blots of R403Q treated for 1 h with DMSO (*D*) or Empa (1 or 50 µM). As control samples a human donor sample (donor) was loaded and an untreated or isoprenalin (Iso, 100 nM) treated control EHT (Ctrl). Almost no phosphorylation of PLB at Ser16 or cMyBP-C at Ser282 was detected in R403Q, in contrast to control samples. Results were identical when GAPDH or α-actinin was used as a loading control (indicated by α-actinin/GAPDH). Blots were cut at 75 kDa and below 20 kDa. Data are expressed as mean ± SEM (*A*: 3 independent EHT preparations; *B*, *C*: two independent EHT preparations; *D*: one EHT preparation; *E*, *F*: three–five EHTs per group). #$P < 0.05$, ##$P < 0.01$, ###$P < 0.001$ vs. (*A*–*D*) Baseline vs. (*E*, *F*) DMSO, (*A*, *B*, *D*) repeated measures one-way ANOVA followed by Dunnett's post-test, or (*C*) if values are missing because EHTs stopped beating as a result of the treatment a mixed-effects analysis followed by Dunnett's post-test was performed, or (*E*, *F*) one-way ANOVA followed by Dunnett's post-test. Abbreviation: M, marker.

Cana (most potent SGLT2i) directly affects and binds to the L-type Ca^{2+} channel. Cana binding to the dihydropyridine site in rat cerebral cortex was detected (*Table 1*, *Figure 7B*) at high concentrations ($IC_{50} = 37$ μM). No binding of Cana to the diltiazem site was detected, and binding to the verapamil site was only detected at 100 μM Cana ($IC_{50} > 100$ μM) in human embryonic kidney 293 (HEK-293) cells (*Table 1*). To investigate if Empa, Cana, and Dapa indirectly block the L-type Ca^{2+} channel, patch clamp experiments were performed in HEK-293 cells. $I_{Ca,L}$ were only inhibited by Cana (*Table 2*) at a high concentration ($IC_{50} > 10$ μM). Therefore, although functional data with diltiazem in EHT suggest that SGLT2i may affect contractility via the L-type Ca^{2+} channel, no evidence was obtained in HEK-293 cells for direct or indirect SGLT2i-effects on the L-type Ca^{2+} channel at clinically relevant concentrations.

NCX: NCX was expressed in R403Q and did not differ from R403Qic (see Supplementary material online, *Figure S12A*). High (see Supplementary material online, *Figure S16A*) and low concentrations (*Figure 7C* and Supplementary material online, *Figure S17A*) of the potent and selective NCX inhibitor SEA0400 reduced relaxation time in R403Q. Similar effects were observed with the reverse-mode NCX inhibitor YM-244769 (see Supplementary material online, *Figure S17B*). Interestingly, SEA0400 treatment in Ctrl EHT increased relaxation time and force (*Figure 7C* and Supplementary material online, *Figure S16B*). Irregular beating patterns (see Supplementary material online, *Figure S17C*) were observed in some R403Q and Ctrl EHTs upon treatment with NCX inhibitors (indicated in the legends of *Figure 7C*, Supplementary material online, *Figures S16 and S17A, B*), which was not observed with SGLT2i. To investigate if NCX activity in R403Q is involved in the SGLT2i-effects on relaxation, R403Q EHTs were pre-treated with SEA0400 (45 min) and subsequently treated with Empa in combination with SEA0400. No additional effect of Empa was observed on relaxation time when Empa treatment was combined with SEA0400 (SEA0400 + Empa) compared to SEA0400 only (SEA0400, *Figure 7E*), whereas Empa treatment alone (Empa) significantly lowered relaxation time compared to baseline. This implies that the acute SGLT2i-effects on relaxation in R403Q depend on NCX activity.

3.6 Unravelling SGLT2i-mediated mechanisms using patch clamp in 2D R92Q-*TNNT2* hiPSC-CMs

To further characterize the potential mechanism(s) of the beneficial effects of SGLT2i, we next performed a series of patch clamp experiments. We therefore used the R92Q-*TNNT2* hiPSC-CMs and tested the effects of Cana because this drug resulted in the most prominent effects in our previous experiments. We focused on the effects of 1, 3, and 10 μmol/L Cana on action potential (AP) measurements, and since effects on APs were only present at 10 μmol/L, we tested subsequently the effects of 10 μmol/L on I_{Na}, I_{NCX}, and $I_{Ca,L}$.

Typical AP examples are shown in *Figure 8A*, top left panel. Application of 10 μmol/L Cana shortened the AP, and this effect was reversible upon wash-out of the drug. The average AP parameters demonstrated that the AP duration shortened significantly at all phases of the repolarization (APD_{20}, APD_{50}, and APD_{90}), but this was only present using 10 μmol/L Cana (*Figure 8A*). Other AP parameters, including maximum diastolic potential, maximal AP amplitude, and maximal AP upstroke velocity, were not affected by Cana (*Figure 8A*); thus, Cana affects only the AP repolarization phase.

Next, we measured I_{Na} during a single depolarizing pulse from −120 to −20 mV. *Figure 8B* shows a typical I_{Na} recording and summarizes the average effects of Cana on peak and late I_{Na}. The typical I_{Na} examples demonstrate a characteristic rapidly activating and inactivating $I_{Na,}$ but neither peak, nor late I_{Na} (measured as the average current of the last 50 ms of the voltage clamp step) was significantly affected by 10 μM Cana. In the absence of Cana, late I_{Na} was 5.1 ± 1.5% ($n = 5$) of the peak I_{Na}, thus confirming the presence of late I_{Na} as found previously in undiseased and diseased hiPSC-CMs lines,[32–34] although our late I_{Na} was quite substantial in agreement with the HCM phenotype.[21] The absence of effects on peak I_{Na} is consistent with the unaltered V_{max}, which is mainly set by the sodium channels.[35]

Subsequently, we recorded the I_{NCX} as $NiCl_2$-sensitive current during a descending ramp in the absence and the presence of 10 μM Cana. *Figure 8C* shows the average current–voltage relationship of I_{NCX} and summarizes the changes in I_{NCX} at +70 and −120 mV. Cana significantly reduced both the reverse (outward) mode and the forward (inward) mode of the I_{NCX}. Interestingly, the reduction was more pronounced at +70 mV, i.e. reverse-mode, compared to the reduction at −120 mV, i.e. forward mode. The effect was reversible (data not shown).

Finally, we tested the effects of 10 μmol/L Cana on $I_{Ca,L}$. *Figure 8D* shows typical recordings upon depolarization steps to 0 mV, and the currents were virtually overlapping in the absence and the presence of Cana, suggesting no effects on amplitude or speed on current inactivation. This is supported by the average findings of the amplitude and time constant (τ) (*Figure 8D*, most left panel). Mean current–voltage relationships of $I_{Ca,L}$ were also overlapping in the absence and the presence of Cana. Furthermore, neither the voltage dependency of activation nor the voltage dependency of inactivation was affected by Cana as can be inferred from the unaffected $V_{1/2}$ and k values (*Figure 8D*).

4. Discussion

We demonstrate that (i) HCM mutations in hiPSC-CMs mimic early features observed in HCM patients; (ii) SGLT2i enhance the relaxation of hiPSC-CMs, to a larger extent in HCM hiPSC-CMs; (iii) effects of Cana > Dapa > Empa; (iv) SGLT2i-effects on relaxation in R403Q EHT depends on culture duration, i.e. hiPSC-CMs maturation; (v) SGLT2i acutely affect Ca^{2+} handling in diseased hiPSC-CMs; and (vi) SGLT2i-mediated effect on relaxation in mutant hiPSC-CMs can be attributed to altered NCX activity.

4.1 HCM mutations in hiPSC-CMs mimic cardiac features of human HCM

Early functional changes described in HCM patients, presenting before hypertrophy, are diastolic dysfunction with either a preserved systolic function or hypercontractility.[4,36] Potentially, studies in hiPSC-CMs allow to investigate the early mutation-induced changes in contractility in a human model, in the absence of secondary disease modifications like neuro-humoral changes or comorbidities (e.g. high blood pressure).[26] In R403Q-*MYH7* EHT force was increased, which is in accordance with the observation that the R403Q mutation causes hypercontractility by increasing the number of functionally accessible myosin heads available to interact with actin.[37] In *TNNT2*-R92Q, hiPSC-CM relaxation was prolonged compared to R92Qic. Our hiPSC-CM models thus mimic early cardiac features of HCM.

4.2 SGLT2i enhances hiPSC-CMs relaxation especially in the presence of a HCM mutation

We observed that acute treatment with SGLT2i improves relaxation in hiPSC-CM 2D and 3D models and that the effect was larger in cells containing an HCM sarcomere mutation compared to controls. The increased efficacy of SGLT2i with pathology seems to be a general characteristic of these drugs,[9] making them ideally suited to treat cardiac diseases. Similarly, Cana was recently shown to induce endothelium-independent relaxation in arteries from human visceral adipose tissue, with larger effects in arteries from obese patients than in controls.[38] In HCM patients and animal models, mutation-specific pathology and treatment responses have been identified.[26] We provide evidence that SGLT2i improve relaxation in hiPSC-CMs harbouring a thick-filament and a thin-filament mutation. As previous clinical and preclinical studies showed a positive effect of chronic SGLT2i treatment on diastolic dysfunction in diabetes and an HFpEF rat model,[16,17,39–41] our data indicates that SGLT2i may also be

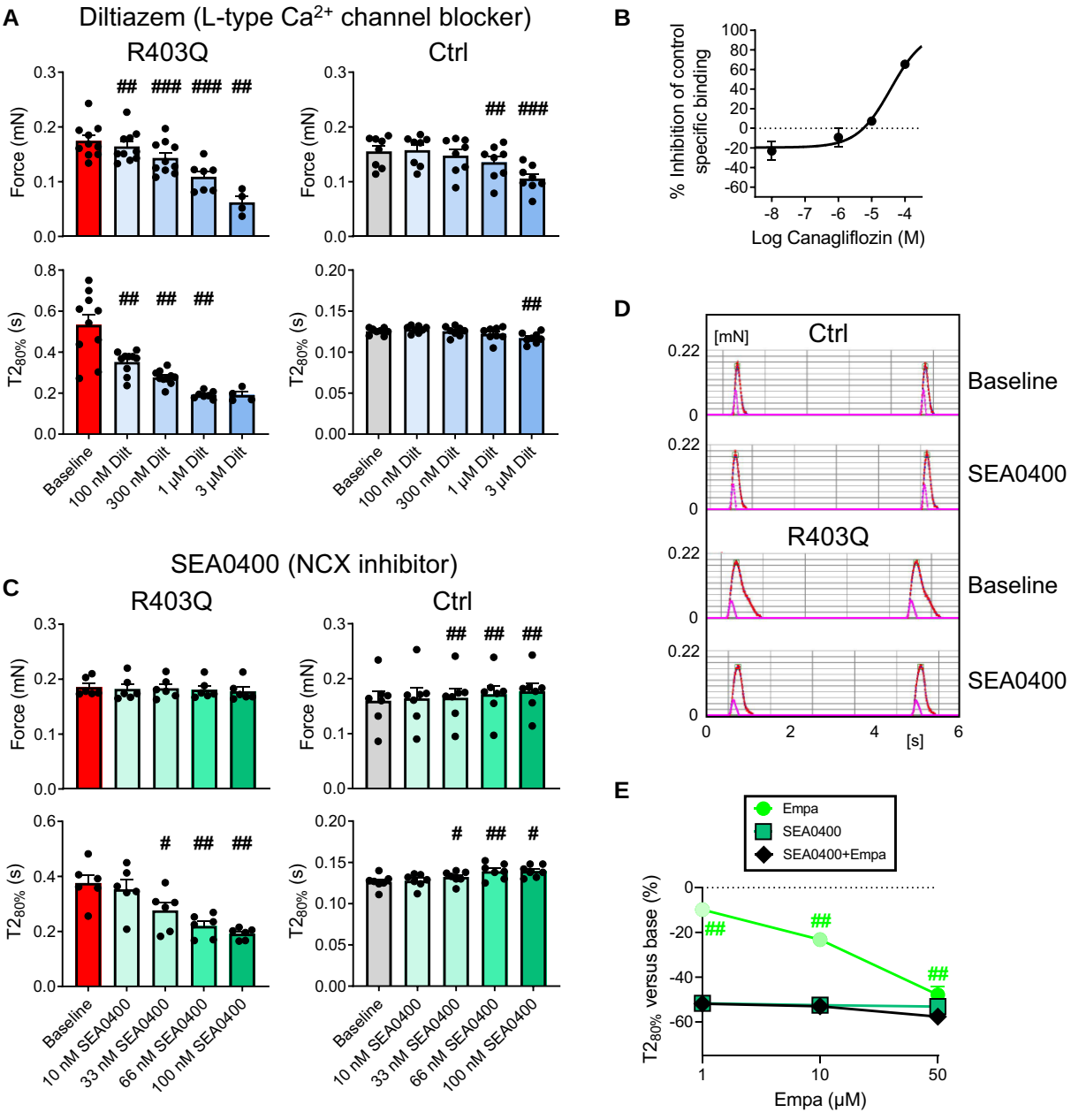

Figure 7 Molecular targets of SGLT2i that enhance relaxation in R403Q EHT. (*A*) Treatment with the L-type Ca^{2+} channel blocker diltiazem hydrochloride (Dilt) for 1 h in spontaneously beating R403Q ($n = 10$, 90 ± 1 days) and Ctrl ($n = 8$, 82 ± 3 days). R403Q EHTs stopped beating at 1 µM Dilt (three EHTs) and 3 µM Dilt (six EHTs). (*B*) The binding affinity of Cana for the dihydropyridine site of the L-type Ca^{2+} channel was determined (two replicates) in the rat cerebral cortex via a radioligand binding assay. Log(inhibitor) vs. response variable slope (four parameters) was fitted with the constraint top is 100. The concentration causing a half-maximal inhibition of control specific binding (IC_{50}) was 37 µM. (*C*) Treatment with the potent NCX inhibitor SEA0400 for 1 h lowered relaxation time of spontaneously beating R403Q ($n = 6$, 56 ± 8 days), whereas SEA0400 increased relaxation time in Ctrl ($n = 7$, 81 ± 2 days). Treatment with SEA0400 resulted in some EHTs in irregular beating patterns (R403Q: 1 EHT at 33 nM; Ctrl: 1 EHT at 100 nM), which were excluded from data analyses. (*D*) Examples of beating patterns of a Ctrl and R403Q EHT with the same beating frequency, before treatment (baseline) and after SEA0400 (100 nM) treatment (red line, original recording; pink line, velocity). (*E*) R403Q EHTs (75 ± 1 days) were cumulatively treated for 45 min with Empa ($n = 6$), or with SEA0400 (100 nM; $n = 6$), or with both SEA0400 (100 nM) and Empa ($n = 8$). At 50 µM Empa two EHTs stopped beating, whereas six EHTs stopped beating at 50 µM Empa + SEA0400. Data are expressed as mean ± SEM. (*A*, *C*: 2 independent EHT preparations of R403Q and Ctrl; *E*: 1 EHT preparation). #$P < 0.05$, ##$P < 0.01$, ###$P < 0.001$ vs. Baseline (*A*, *C*, *E*: Empa) or vs. SEA0400 (*E*: SEA0400 + Empa), repeated measures one-way ANOVA followed by Dunnett's post-test (*A*: Ctrl, C), or if values are missing because EHTs stopped beating as a result of the treatment a mixed-effects analysis followed by Dunnett's post-test was performed (*A*: R403Q, *E*: Empa vs. baseline), or one-way ANOVA followed by Tukey's multiple comparisons tests (*E*: SEA0400 vs. SEA0400 + Empa).

Table 1 Canagliflozin binding to three binding sites of the L-type Ca^{2+} channel

	Inhibition of control specific binding (%)								
	Dihydropyridine site			Diltiazem site			Verapamil site		
[Cana]	1st	2nd	Mean	1st	2nd	Mean	1st	2nd	Mean
10 nM	−32.5	−13.7	−23.1	1.8	−1.8	0.0	−3.6	−0.5	−2.1
100 nM	−64.4[a]	−45.9[a]	−55.2[a]	0.9	−3.3	−1.2	7.0	10.4	8.7
1 μM	0.3	−18.7	−9.2	−8.4	−1.8	−5.1	7.5	−6.0	0.8
10 μM	10.4	4.3	7.4	−19.1	−14.4	−16.8	1.4	−11.9	−5.3
100 μM	69.6	61.1	65.4	1.2	−27.8	−13.3	23.6	40.1	31.9

Cana binding (five concentrations, two replicates) to three different binding sites of the L-type Ca^{2+} channel was investigated via binding assays. Cana binding to the dihydropyridine site was detected at high concentrations with an IC_{50} value (concentration causing a half-maximal inhibition of control specific binding) of 37 μM, a Hill coefficients of 0.9, and a K_i of 19 μM. Cana did not bind to the diltiazem site. Cana binding to the verapamil site of the L-type Ca^{2+} channel was only detected at 100 μM (IC_{50} > 100 μM). An inhibition >50% represents a significant effect and between 25 and 50% a weak to moderate effect. Inhibition (or stimulation) <25% is not considered significant and mostly attributable to variability of the signal around the control level.
[a]Outlier, quality criteria and the definition of an outlier according to Eurofins: the 'bottom' experimental plateau is considered to be consistent when it is between −25 and 25%. The value at 100 nM Cana (−55.2%) is far from the experimental plateau (−20%) and is therefore considered an 'outlier' and was excluded from IC_{50} calculation.

Table 2 L-type Ca^{2+} channel patch clamp assay

	Inhibition (%)								
	Empagliflozin			Canagliflozin			Dapagliflozin		
[SGLT2i]	1st	2nd	Mean	1st	2nd	Mean	1st	2nd	Mean
0.1 μM	−3.0	6.2	1.6	9.5	−3.3	3.1	15.5	18.8	17.2
0.3 μM	11.4	15.2	13.3	18.5	−1.3	8.6	13.9	16.5	15.2
1 μM	2.0	10.3	6.2	6.9	5.0	6.0	−5.3	5.9	0.3
3 μM	6.0	14.7	10.4	18.8	18.7	18.8	−10.2	7.2	−1.5
10 μM	13.4	7.7	10.6	31.7	30.2	31.0	−12.6	8.4	−2.1

Electrophysiological assays were conducted to profile empagliflozin, canagliflozin, and dapagliflozin (five concentrations and two replicates) for activities on the L-type Ca^{2+} channel using the QPatch electrophysiological platform (Eurofins). Results showing an inhibition higher than 50% are considered to represent significant effects of test compounds. IC_{50} values of empagliflozin and dapagliflozin could not be calculated, since no inhibition >25% was observed. For canagliflozin, the estimated IC_{50} > 10 μM. For the reference compound nifedipine, an IC_{50} value of 0.30 μM was calculated.

effective in the treatment of HCM. Our results in cultured heart muscle also indicate that the SGLT2i-mediated enhanced relaxation *in vivo* is a direct cardiac effect that is (at least partly) independent of systemic changes. With respect to force, acute negative inotropic effects of Dapa (1 μM) have been reported in isolated control and diabetic rat cardiomyocytes.[15] We observed that Empa and Cana slightly but significantly reduced force in R403Q EHT, which may be beneficial since these muscles are hypercontractile.

4.3 Comparison of acute effects of Empa, Cana, and Dapa on cardiac function

Different SGLT2i are used in the clinic with varying SGLT type 2 over type 1 selectivity: Empa: 2680-fold; Dapa: 1242-fold; Cana: 155-fold.[20] It is not known whether SGLT2i are interchangeable or if specific SGLT2i offer unique benefits or harm in specific clinical settings.[42] Differences between SGLT2i in effectiveness for the prevention of heart failure hospitalization have been reported, however, highly variable outcomes were also observed for SGLT2i that completed more than one trial.[42,43] So far, the available data of clinical trials does not clearly show that one SGLT2i is superior over the others, so both the benefit and the side effects may be part of SGLT2i class features.[42,43] Our study shows that the SGLT2i-enhanced relaxation is a class effect, at low concentration (1 μM), although the effect size differs, i.e. Cana > Dapa > Empa. Our comparison of different SGLT2i may be helpful to understand the outcome of future randomized clinical trials in which different SGLT2i are directly compared.

4.4 SGLT2i-enhanced relaxation in R403Q EHTs depends on culture duration

We observed that prolonged culturing of R403Q EHTs increased hiPSC-CMs maturity and enhanced SGLT2i-mediated relaxation. Similar effects of prolonged hiPSC-CMs culturing have been shown for drug responses to β-adrenergic stimulation.[44] More mature phenotypes in morphology, structure, and physiology after prolonged hiPSC-CMs culture time have been reported.[45] Prolonged hiPSC-CMs culturing is important for future SGLT2i-studies, since we only observed effects on contractility at 1 μM Empa and Dapa after prolonged culturing. Alternatively, other cues can be used for hiPSC-CMs maturation, such as hormones, alterations in energy source, and/or electrical stimulation.[45]

4.5 SGLT2i acutely affect Ca^{2+} handling in 2D cultured diseased hiPSC-CMs

Our study shows that SGLT2i acutely affect Ca^{2+} handling in 2D cultured HCM hiPSC-CMs. No significant acute effects of Empa on Ca^{2+} handling were observed in control hiPSC-CMs cultured for 28 days. Similarly, chronic Empa (0.5 μM) treatment for 2 or 8 weeks did not affect excitation-contraction-coupling and electrophysiology in non-diseased

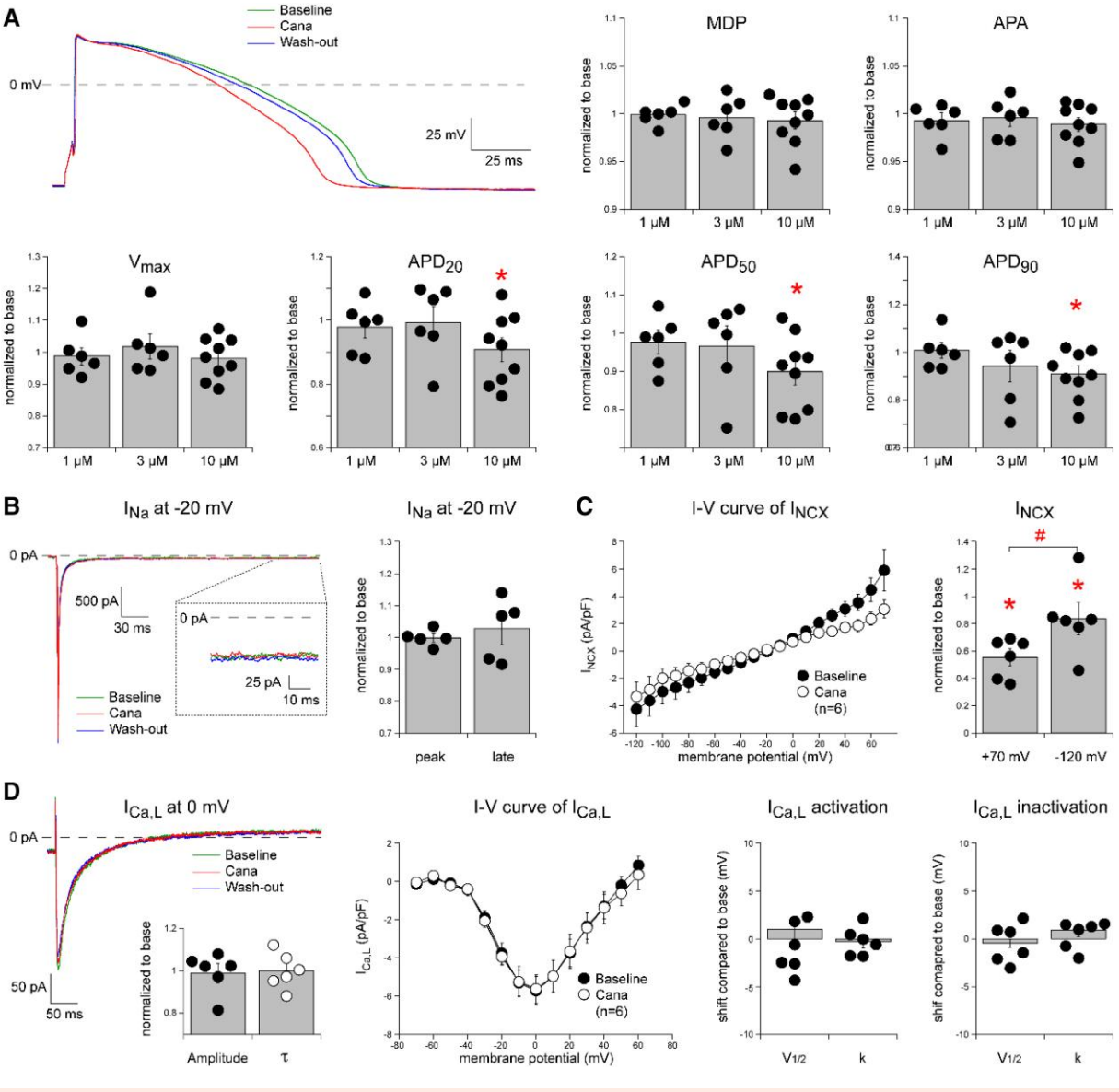

Figure 8 Effects of Cana on APs and membrane currents in *TNNT2*-R92Q hiPSC-CM. (*A*) Typical APs in the absence and the presence of 10 µmol/L Cana and average effects (depicted as dot plots) of 1, 3, and 10 µmol/L Cana on AP parameters. MDP = maximum diastolic potential, APA = maximal AP amplitude, V_{max} = maximal AP upstroke velocity, and APD_{20}, APD_{50}, APD_{90} = AP duration at 20, 50, and 90% of repolarization. (*B*) Typical sodium currents (I_{Na}), evoked by 300 ms depolarizing pulses from −120 to −20 mV, in the absence and the presence of 10 µmol/L Cana. The dot plots show the average effects on peak and late I_{Na}. (*C*) Current–voltage (*I–V*) relationships of the Na^+/Ca^{2+} exchange current (I_{NCX}) in the absence and the presence of 10 µmol/L Cana. I_{NCX} was measured during a descending ramp as a $NiCl_2$-sensitive current. The dot plots indicate that I_{NCX} was significantly affected by Cana, with a more pronounced reduction at +70 mV, i.e. reverse-mode of I_{NCX}, than at −120 mV, i.e. the forward mode (D). Typical L-type Ca^{2+} current ($I_{Ca,L}$), evoked by 500 ms depolarizing pulses from −60 to 0 mV, in the absence and the presence of 10 µmol/L Cana. Neither the amplitude nor the time constant (τ) of current inactivation was significantly affected. $I_{Ca,L}$ was also not affected at other potential, as shown in the average *I–V* relationships, and the voltage dependency of (in)activation was similar in the absence and presence of Cana. Voltage dependence of activation and inactivation curves were fitted with the Boltzmann function $y = [1 + \exp\{(V\text{-}V_{1/2})/k\}]^{-1}$ to determine half-maximal voltage ($V_{1/2}$; in mV) of (in) activation and the slope factor (k; in mV). *$P < 0.05$ (paired *t*-test).

hiPSC-CMs.[46] We show in human R403Q iPSC-CMs that SGLT2i within 15 min lowered the Ca^{2+} transient amplitude, peak time, and decay time, with larger Cana effects compared to Empa. Cana also lowered the Ca^{2+} transient amplitude in *TNNT2*-R92Q hiPSC-CMs. Previous studies also showed that 1 µM Empa acutely lowers cytoplasmic Ca^{2+} in cardiomyocytes from healthy rabbits and that 1 µM Dapa reduced the Ca^{2+} transient amplitude in diabetic rat cardiomyocytes.[11,15] In hiPSC-CMs exposed to high glucose for 2 weeks, chronic Empa (5 µM) also lowered the Ca^{2+} amplitude and increased the maximal decay velocity of Ca^{2+} transients.[47]

A reduction in cytosolic [Ca^{2+}] upon SGLT2i treatment is expected to affect CaMKII activity. CaMKII is autophosphorylated upon elevated [Ca^{2+}] at Thr286, which renders it constitutively active and which may

favour myocardial dysfunction. In line with this, chronic Empa treatment in diabetic mice improved diastolic dysfunction and decreased CaMKII phosphorylation at Thr286 and its activation.[39] We did not observe any differences in CaMKII-Thr286 phosphorylation between R403Qic and R403Q (see Supplementary material online, *Figure S12B*), and acute Empa treatment of R403Q did not affect CaMKII-Thr286 phosphorylation (see Supplementary material online, *Figure S14B*). This is in accordance with a report in which Empa after 24 h potently reduced CaMKII activity in murine cardiomyocytes, but not after 30 min in human failing ventricular tissue.[48]

Empa pre-treatment (1 μM) has also been shown to decrease the lipopolysaccharide-induced increase in intracellular Ca^{2+} in human fetal ventricular cardiomyocytes (RL-14 cell line).[49] Interestingly, the ability of Empa to reduce inflammation was completely blunted by a Ca^{2+} ionophore, suggesting that Empa exerted its benefit upon restoring the optimal cytoplasmic Ca^{2+} levels in the heart. Our data shows that the SGLT2i-mediated changes in contractile function are related to changes in Ca^{2+} handling in HCM hiPSC-CMs. It could be speculated that SGLT2-effects on metabolism, oxidative stress, inflammation, and contractility are all indirect effects of SGLT2-mediated changes in intracellular [Ca^{2+}]. Many disease states increase intracellular [Ca^{2+}], which may explain the larger SGLT2i-mediated effects in disease models.

4.6 Molecular targets of SGLT2i that enhance relaxation in mutant hiPSC-CMs

Identifying the molecular target of the SGLT2i-enhanced relaxation in mutant hiPSC-CMs provides information about the SGLT2i working mechanism and also informs about the early HCM pathology. SGLT2i were originally developed as a glucose-lowering antidiabetic drug that inhibits the SGLT2 and thereby glucose reabsorption in the proximal tubule, promoting urinary glucose excretion. We did not detect SGLT2 expression in human EHT and Empa also reduced relaxation time in glucose-free conditions. These observations in R403Q suggest that the Empa effects on relaxation are independent of SGLT activity. This is in line with our previous study, showing that Empa reduced infarct size independently of SGLT2.[50] Interestingly, the SGLT2i off-target effects so far identified in cardiomyocytes have also been implicated in HCM pathology. Below, we will discuss these SGLT2i-targets, their role in HCM, and the potential involvement in the SGLT2i-enhanced relaxation in mutant hiPSC-CM models.

NHE-1: Increased NHE-1 expression was found in an HCM mouse model with a mutation in α-tropomyosin.[24] An important off-target effect of SGLT2i is NHE-1 inhibition, which was first demonstrated by using the selective NHE-1 inhibitor cariporide.[11,12] Similarly, we tested if cariporide lowers relaxation time. However, cariporide did not reduce force and relaxation time at 1 and 10 μM in R403Q, while it has been demonstrated that 10 μM cariporide fully inhibits NHE-1 in rat cardiomyocytes.[51] Only at 50 μM cariporide, a relatively small reduction in relaxation time was observed in R403Q. NHE-1 inhibition by SGLT2i has been a matter of intense debate, since not all studies identified SGLT2i as NHE-1 inhibitors.[52–56] When taking into account that cariporide is a very potent NHE-1 inhibitor, our results suggest that the Empa effects on relaxation in R403Q were not mediated by only inhibiting NHE-1.

$Na_v1.5$: An enhanced $I_{Na\text{-}Late}$ has been demonstrated as an important contributor to electrophysiological and intracellular Ca^{2+} handling abnormalities in HCM patients.[21] SGLT2i are potent $I_{Na\text{-}Late}$ inhibitors and thus may be beneficial in HCM.[10,13] We show that the $Na_v1.5$ antagonist and $I_{Na\text{-}Late}$ inhibitor ranolazine hydrochloride did not lower relaxation time in R403Q, which implies that the SGLT2i-enhanced relaxation was not mediated by inhibiting $Na_v1.5$. This is in accordance with the finding that Cana ($IC_{50} = 1.26$ μM) is less potent compared to Empa ($IC_{50} = 0.79$ μM) and Dapa ($IC_{50} = 0.58$ μM) with respect to $I_{Na\text{-}Late}$-inhibition, whereas Cana in R403Q was the most potent SGLT2i with respect to muscle relaxation.[10] This is also in line with a recent clinical trial in which ranolazine treatment of patients with non-obstructive HCM did not ameliorate functional impairment related to diastolic dysfunction.[57] Our patch clamp studies confirmed that Cana does not alter I_{Na} in mutant hiPSC-CMs.

ROS/NO: Excessive cellular ROS levels in HCM have been reported, which may impair cardiomyocyte relaxation.[4] Empa lowered oxidative stress in diabetes and in HFpEF.[13,14] We therefore investigated if antioxidants have similar effects on R403Q relaxation as SGLT2i. Both the mitochondrial antioxidant SS-31 and the antioxidant NAC did not affect relaxation. Lowering ROS levels will increase NO bioavailability and since Empa has been reported to increase NO bioavailability, we also investigated NO involvement.[58] Relaxation time was reduced by Empa in both the absence and the presence of the NO inhibitor L-Name. It is therefore unlikely that the acute Empa effects on relaxation in R403Q were only mediated by changes in ROS or NO.

PLB/cTnI/cMyBP-C phosphorylation: Phosphorylation of PLB and cTnI enhances cardiac muscle relaxation via increased sarcoplasmic reticulum Ca^{2+} pumping and via an increased rate of Ca^{2+} dissociation from the myofilaments, respectively.[18] In addition, phosphorylation of cMyBP-C may also enhance relaxation.[19] In HCM patients with sarcomere mutations, phosphorylation of cTnI and cMyBP-C was reduced compared to donor samples.[25] Interestingly, Empa was shown to reduce inflammation and oxidative stress in HFpEF and improve protein kinase G (PKG)Ia activity, increasing phosphorylation levels of cTnI-Ser23/24 and with less effect on cMyBP-C-Ser282.[14,16] Chronic Empa was also shown to increase PLB phosphorylation in a mouse model of diabetes and improved diastolic function.[17] We therefore investigated if these post-translational modifications underlie the improved relaxation in R403Q. However, we did not observe an increase in phosphorylation of PLB-Ser16/Thr17, cTnI-Ser23/24, and cMyBP-C-Ser282 in R403Q upon Empa treatment, which is in line with other studies in different disease models.[39,40,47,48]

L-type Ca^{2+} channel: $I_{Ca,L}$ is increased in cardiomyocytes from HCM patients and in HCM hiPSC-CMs.[21,59,60] Furthermore, the L-type Ca^{2+} channel blocker diltiazem prevented diastolic heart failure in HCM mice (TnT-I79N) and improved mean left ventricular end-diastolic diameter in preclinical HCM mutation carriers.[23,61] SGLT2i may target the L-type Ca^{2+} channel since acute exposure to 1 μM Dapa has been shown to reduce the amplitude of $I_{Ca,L}$ in rat cardiomyocytes.[15] Interestingly, we show that diltiazem has similar acute effects as SGLT2i on force and relaxation in R403Q and in Ctrl. However, our study shows no evidence of direct or indirect effects of SGLT2i on the L-type Ca^{2+} channel in HEK-293 cells via binding and patch clamp assays. In addition, our patch clamp studies in mutant hiPSC-CMs showed no effect of Cana on $I_{Ca,L}$.

NCX: NCX maintains Ca^{2+} homeostasis in cardiomyocytes as it primarily removes Ca^{2+} (forward mode) that enters through the L-type Ca^{2+} channel on a beat-to-beat basis. However, under pathological conditions, reverse-mode NCX is enhanced (Ca^{2+} influx). In HCM myocardium and HCM hiPSC-CMs, the NCX forward-mode activity is reduced.[21,62] HCM mutations may promote reverse NCX activity via enhanced $I_{Na\text{-}Late}$, increased $I_{Ca,L}$, and AP prolongation, as NCX only effectively works in forward mode at diastolic potentials.[21] Interestingly, SGLT1&2i may positively affect NCX function in HCM, as chronic treatment of HFpEF rats with sotagliflozin increased forward-mode NCX activity.[20] SGLT2i may be hypothesized to directly affect/bind NCX since SGLT2i acutely affect Ca^{2+} handling and since all SGLT2i-targets so far are also Na^+ channels (SGLT2, NHE-1, Nav1.5). However, acute Empa (1 μM) application did not significantly inhibit reverse-mode NCX1.1 in HEK293T cells overexpressing NCX1.1.[10] Alternatively, SGLT2i may indirectly affect NCX activity by shortening the AP duration via other ion channels like voltage-dependent repolarizing K^+ currents.[63] Our data support that altered NCX activity underlies the SGLT2i-enhanced relaxation in mutant hiPSC-CM models. This is evident from (i) the opposite effects on contractility observed with SEA0400 in Ctrl and HCM EHT; (ii) the low concentrations (33 nM) of both NCX inhibitors that affected contractility, which makes off-target effects less likely; (iii) the effects on contractility in R403Q EHT with the reverse-mode NCX inhibitor YM-244769; (iv) the acute SGLT2i-effects on Ca^{2+} handling in R403Q; (v) the observation that Empa did not affect relaxation in R403Q EHT in combination with SEA0400, i.e. SGLT2i-effects on relaxation in R403Q depended on NCX activity, and finally, (vi) the Cana-mediated change in NCX activity in patch clamp experiments in R92Q-*TNNT2* hiPSC-CMs.

To conclude about the molecular mechanism, like statins, the SGLT2i exert pleiotropic effects, exerting multiple pharmacological activities. Besides inhibiting SGLT2, previous studies have demonstrated that SGLT2i directly inhibit the ion channels NHE-1 and $Na_v1.5$, lowering intracellular Na^+ and Ca^{2+} levels in cardiomyocytes. Our data with specific inhibitors of NHE-1 and $Na_v1.5$ show that SGLT2is-mediated inhibition of only NHE-1 or only $Na_v1.5$ did not enhance relaxation in R403Q EHT. A combination of the inhibition of NHE-1 or $Na_v1.5$ with other SGLT2i-effects (e.g. lowering oxidative stress, affecting K^+-channels or an unknown target) or a combination of the inhibition of both NHE-1 and $Na_v1.5$ by SGLT2i may have caused the enhanced relaxation in R403Q EHT. Previous studies also reported on SGLT2i-effects on the L-type Ca^{2+} channel and NCX activity. We showed that the L-type Ca^{2+} channel is not a direct target of SGLT2i. However, based on our functional data with diltiazem, indirect inhibition of the L-type Ca^{2+} channel upon SGLT2i treatment may have contributed to the SGLT2i-mediated enhanced relaxation in R403Q EHT. Overall, our data indicate that altered NCX activity underlies the acute SGLT2i-enhanced relaxation in mutant hiPSC-CMs.

4.7 Limitations of hiPSC-derived models

We used a well-validated EHT system to study the effects of SGLT2i.[27,28] In the current study, we however did not measure sarcomere length and cross-sectional area of cardiomyocytes. We thus cannot exclude an effect of differences in sarcomere length between different cell lines. However, our protocol resulted in highly reproducible data for each cell line, similar EHT width (*Figure 2B*) and consistent SGLT2i-mediated effects both in 2D and in 3D hiPSC-CMs. Moreover, drug effects were studied in the same preparations.

The EHTs in the present study were not chronically paced during culture. Improved maturation of EHTs has been described using continuous pacing during culture;[64] however, chronic pacing may also be harmful and introduce adverse structural and electrophysiological changes.[65] While resting beating frequency differed between control and mutant EHTs, the effects of SGLT2i cannot be attributed to differences in beating frequency as drug effects were present under paced conditions. Moreover, while the beating rate decreased in the initial days of culture, it remained stable for >40 days (*Figure 4B*). Thus, we exclude that the more pronounced effects of SGLT2i at prolonged culturing are due to differences in baseline beating rate.

In some experiments, we applied a very high concentration of SGLT21, i.e. 50 μM, which is not pharmacologically relevant. A review on the reproducibility of science,[66] indicated that determination of drug dose-response is one of the essential aspects required for accurate pharmacology studies, which is why we do believe that providing the full dataset adds to the robustness of our study.

Finally, we have performed patch clamp experiments in single R92Q-*TNNT2* hiPSC-derived cardiomyocytes instead of cells isolated from EHTs. So far, there are no indications that the gating properties and modulation of ion channels and exchangers are different between monolayers and EHT-grown cells,[67–70] except for norepinephrine effects on L-type Ca^{2+} current.[70] Differences in current density between monolayers and EHT-grown cells are known, but this will not affect the percentage changes of drugs. In addition, the APs were measured using a dynamic clamp injected Kir2.1 current and have a physiological resting membrane potential of around −80 mV. Thus, ion channels have had a normal physiological availability.

Translational perspective

Hypertrophic cardiomyopathy (HCM) is the most common inherited cardiomyopathy and treatment to prevent mutation-induced cardiac dysfunction is lacking. Early HCM characteristics are diastolic dysfunction and hypercontractility. We show in hiPSC-CM models that SGLT2i represents a potential therapy to correct cardiomyocyte dysfunction induced by HCM sarcomere mutations. SGLT2i acutely enhanced relaxation and altered Ca^{2+} handling in HCM hiPSC-CMs, targeting important early HCM disease hallmarks.

5. Conclusion

HCM mutations in hiPSC-CMs mimic the early features observed in HCM patients. SGLT2i enhance the relaxation of hiPSC-CMs, and the effects were larger in HCM hiPSC-CMs compared to Ctrl. Cana effects on relaxation are more pronounced than Empa and Dapa, and these effects depend on culture duration, i.e. EHT maturation. SGLT2i acutely affect Ca^{2+} handling in diseased hiPSC-CMs, which is mediated via altered NCX activity. SGLT2i are a potential therapy to correct cardiac dysfunction in HCM.

Supplementary material

Supplementary material is available at Cardiovascular Research online.

Acknowledgements

We thank Rio P. Juni for providing the HEK293 lysate and Maike Schuldt for providing the donor lysate for the western blots. We would like to acknowledge the technical assistance of Hans Baltzer and Farzana Mohammad.

Conflict of interest: none declared.

Funding

This work was supported by the Netherlands Cardiovascular Research Initiative: An initiative with the support of the Dutch Heart Foundation (CVON2014-40 DOSIS); and the 91818602 VICI grant, and the Dutch Heart Foundation (2018T010).

Data availability

The authors declare that all data underlying this article are available in the article and in its online supplement.

References

1. Authors/Task Force Members; Elliott PM, Anastasakis A, Borger MA, Borggrefe M, Cecchi F, Charron P, Hagege AA, Lafont A, Limongelli G, Mahrholdt H, McKenna WJ, Mogensen J, Nihoyannopoulos P, Nistri S, Pieper PG, Pieske B, Rapezzi C, Rutten FH, Tillmanns C, Watkins H. 2014 ESC Guidelines on diagnosis and management of hypertrophic cardiomyopathy: the task force for the diagnosis and management of hypertrophic cardiomyopathy of the European society of cardiology (ESC). *Eur Heart J* 2014;**35**:2733–2779.
2. Semsarian C, Ingles J, Maron MS, Maron BJ. New perspectives on the prevalence of hypertrophic cardiomyopathy. *J Am Coll Cardiol* 2015;**65**:1249–1254.
3. Ho CY, Charron P, Richard P, Girolami F, Van Spaendonck-Zwarts KY, Pinto Y. Genetic advances in sarcomeric cardiomyopathies: state of the art. *Cardiovasc Res* 2015;**105**:397–408.
4. Wijnker PJM, Sequeira V, Kuster DWD, Velden JV. Hypertrophic cardiomyopathy: a vicious cycle triggered by sarcomere mutations and secondary disease hits. *Antioxid Redox Signal* 2019;**31**:318–358.
5. Tardiff JC, Carrier L, Bers DM, Poggesi C, Ferrantini C, Coppini R, Maier LS, Ashrafian H, Huke S, van der Velden J. Targets for therapy in sarcomeric cardiomyopathies. *Cardiovas Res* 2015;**105**:457–470.
6. Zannad F, Ferreira JP, Pocock SJ, Anker SD, Butler J, Filippatos G, Brueckmann M, Ofstad AP, Pfarr E, Jamal W, Packer M. SGLT2 inhibitors in patients with heart failure with reduced ejection fraction: a meta-analysis of the EMPEROR-reduced and DAPA-HF trials. *Lancet* 2020;**396**:819–829.

7. Zelniker TA, Wiviott SD, Raz I, Im K, Goodrich EL, Bonaca MP, Mosenzon O, Kato ET, Cahn A, Furtado RHM, Bhatt DL, Leiter LA, McGuire DK, Wilding JPH, Sabatine MS. SGLT2 inhibitors for primary and secondary prevention of cardiovascular and renal outcomes in type 2 diabetes: a systematic review and meta-analysis of cardiovascular outcome trials. *Lancet* 2019;**393**:31–39.
8. Anker SD, Butler J, Filippatos G, Ferreira JP, Bocchi E, Bohm M, Brunner-La Rocca HP, Choi DJ, Chopra V, Chuquiure-Valenzuela E, Giannetti N, Gomez-Mesa JE, Janssens S, Januzzi JL, Gonzalez-Juanatey JR, Merkely B, Nicholls SJ, Perrone SV, Pina IL, Ponikowski P, Senni M, Sim D, Spinar J, Squire I, Taddei S, Tsutsui H, Verma S, Vinereanu D, Zhang J, Carson P, Lam CSP, Marx N, Zeller C, Sattar N, Jamal W, Schnaidt S, Schnee JM, Brueckmann M, Pocock SJ, Zannad F, Packer M; EMPEROR-Preserved Trial Investigators. Empagliflozin in heart failure with a preserved ejection fraction. *N Engl J Med* 2021;**385**:1451–1461.
9. Chen S, Coronel R, Hollmann MW, Weber NC, Zuurbier CJ. Direct cardiac effects of SGLT2 inhibitors. *Cardiovasc Diabetol* 2022;**21**:45.
10. Philippaert K, Kalyaanamoorthy S, Fatehi M, Long W, Soni S, Byrne NJ, Barr A, Singh J, Wong J, Palechuk T, Schneider C, Darwesh AM, Maayah ZH, Seubert JM, Barakat K, Dyck JRB, Light PE. Cardiac late sodium channel current is a molecular target for the sodium/glucose cotransporter 2 inhibitor empagliflozin. *Circulation* 2021;**143**:2188–2204.
11. Baartscheer A, Schumacher CA, Wust RC, Fiolet JW, Stienen GJ, Coronel R, Zuurbier CJ. Empagliflozin decreases myocardial cytoplasmic Na(+) through inhibition of the cardiac na(+)/H(+) exchanger in rats and rabbits. *Diabetologia* 2017;**60**:568–573.
12. Uthman L, Baartscheer A, Bleijlevens B, Schumacher CA, Fiolet JWT, Koeman A, Jancev M, Hollmann MW, Weber NC, Coronel R, Zuurbier CJ. Class effects of SGLT2 inhibitors in mouse cardiomyocytes and hearts: inhibition of Na(+)/H(+) exchanger, lowering of cytosolic Na(+) and vasodilation. *Diabetologia* 2018;**61**:722–726.
13. Lee TI, Chen YC, Lin YK, Chung CC, Lu YY, Kao YH, Chen YJ. Empagliflozin attenuates myocardial sodium and calcium dysregulation and reverses cardiac remodeling in streptozotocin-induced diabetic rats. *Int J Mol Sci* 2019;**20**:1680.
14. Kolijn D, Pabel S, Tian Y, Lodi M, Herwig M, Carrizzo A, Zhazykbayeva S, Kovacs A, Fulop GA, Falcao-Pires I, Reusch PH, Linthout SV, Papp Z, van Heerebeek L, Vecchione C, Maier LS, Ciccarelli M, Tschope C, Mugge A, Bagi Z, Sossalla S, Hamdani N. Empagliflozin improves endothelial and cardiomyocyte function in human heart failure with preserved ejection fraction via reduced pro-inflammatory-oxidative pathways and protein kinase Galpha oxidation. *Cardiovasc Res* 2021;**117**:495–507.
15. Hamouda NN, Sydorenko V, Qureshi MA, Alkaabi JM, Oz M, Howarth FC. Dapagliflozin reduces the amplitude of shortening and Ca(2+) transient in ventricular myocytes from streptozotocin-induced diabetic rats. *Mol Cell Biochem* 2015;**400**:57–68.
16. Pabel S, Wagner S, Bollenberg H, Bengel P, Kovacs A, Schach C, Tirilomis P, Mustroph J, Renner A, Gummert J, Fischer T, Van Linthout S, Tschope C, Streckfuss-Bomeke K, Hasenfuss G, Maier LS, Hamdani N, Sossalla S. Empagliflozin directly improves diastolic function in human heart failure. *Eur J Heart Fail* 2018;**20**:1690–1700.
17. Hammoudi N, Jeong D, Singh R, Farhat A, Komajda M, Mayoux E, Hajjar R, Lebeche D. Empagliflozin improves left ventricular diastolic dysfunction in a genetic model of type 2 diabetes. *Cardiovasc Drugs Ther* 2017;**31**:233–246.
18. Li L, Desantiago J, Chu G, Kranias EG, Bers DM. Phosphorylation of phospholamban and troponin I in beta-adrenergic-induced acceleration of cardiac relaxation. *Am J Physiol Heart Circ Physiol* 2000;**278**:H769–H779.
19. Rosas PC, Liu Y, Abdalla MI, Thomas CM, Kidwell DT, Dusio GF, Mukhopadhyay D, Kumar R, Baker KM, Mitchell BM, Powers PA, Fitzsimons DP, Patel BG, Warren CM, Solaro RJ, Moss RL, Tong CW. Phosphorylation of cardiac myosin-binding protein-C is a critical mediator of diastolic function. *Circ Heart Fail* 2015;**8**:582–594.
20. Bode D, Semmler L, Wakula P, Hegemann N, Primessnig U, Beindorff N, Powell D, Dahmen R, Ruetten H, Oeing C, Alogna A, Messroghli D, Pieske BM, Heinzel FR, Hohendanner F. Dual SGLT-1 and SGLT-2 inhibition improves left atrial dysfunction in HFpEF. *Cardiovasc Diabetol* 2021;**20**:7.
21. Coppini R, Ferrantini C, Yao L, Fan P, Del Lungo M, Stillitano F, Sartiani L, Tosi B, Suffredini S, Tesi C, Yacoub M, Olivotto I, Belardinelli L, Poggesi C, Cerbai E, Mugelli A. Late sodium current inhibition reverses electromechanical dysfunction in human hypertrophic cardiomyopathy. *Circulation* 2013;**127**:575–584.
22. Robinson P, Liu X, Sparrow A, Patel S, Zhang YH, Casadei B, Watkins H, Redwood C. Hypertrophic cardiomyopathy mutations increase myofilament Ca(2+) buffering, alter intracellular Ca(2+) handling, and stimulate Ca(2+)-dependent signaling. *J Biol Chem* 2018;**293**:10487–10499.
23. Ho CY, Lakdawala NK, Cirino AL, Lipshultz SE, Sparks E, Abbasi SA, Kwong RY, Antman EM, Semsarian C, Gonzalez A, Lopez B, Diez J, Orav EJ, Colan SD, Seidman CE. Diltiazem treatment for pre-clinical hypertrophic cardiomyopathy sarcomere mutation carriers: a pilot randomized trial to modify disease expression. *JACC Heart Fail* 2015;**3**:180–188.
24. Al Moamen NJ, Prasad V, Bodi I, Miller ML, Neiman ML, Lasko VM, Alper SL, Wieczorek DF, Lorenz JN, Shull GE. Loss of the AE3 anion exchanger in a hypertrophic cardiomyopathy model causes rapid decompensation and heart failure. *J Mol Cell Cardiol* 2011;**50**:137–146.
25. Sequeira V, Wijnker PJM, Nijenkamp LLAM, Kuster DWD, Najafi A, Witjas-Paalberends ER, Regan JA, Boontje N, ten Cate FJ, Germans T, Carrier L, Sadayappan S, van Slegtenhorst MA, Zaremba R, Foster DB, Murphy AM, Poggesi C, dos Remedios C, Stienen GJM, Ho CY, Michels M, van der Velden J. Perturbed length-sependent activation in human hypertrophic cardiomyopathy with missense sarcomeric gene mutations. *Circ Res* 2013;**112**:1491–1505.
26. Wijnker PJM, van der Velden J. Mutation-specific pathology and treatment of hypertrophic cardiomyopathy in patients, mouse models and human engineered heart tissue. *Biochim Biophys Acta Mol Basis Dis* 2020;**1866**:165774.
27. Hansen A, Eder A, Bonstrup M, Flato M, Mewe M, Schaaf S, Aksehirlioglu B, Schwoerer AP, Uebeler J, Eschenhagen T. Development of a drug screening platform based on engineered heart tissue. *Circ Res* 2010;**107**:35–44.
28. Wijnker PJ, Friedrich FW, Dutsch A, Reischmann S, Eder A, Mannhardt I, Mearini G, Eschenhagen T, van der Velden J, Carrier L. Comparison of the effects of a truncating and a missense MYBPC3 mutation on contractile parameters of engineered heart tissue. *J Mol Cell Cardiol* 2016;**97**:82–92.
29. Saleem U, van Meer BJ, Katili PA, Mohd Yusof NAN, Mannhardt I, Garcia AK, Tertoolen L, de Korte T, Vlaming MLH, McGlynn K, Nebel J, Bahinski A, Harris K, Rossman E, Xu X, Burton FL, Smith GL, Clements P, Mummery CL, Eschenhagen T, Hansen A, Denning C. Blinded, multicenter evaluation of drug-induced changes in contractility using human-induced pluripotent stem cell-derived cardiomyocytes. *Toxicol Sci* 2020;**176**:103–123.
30. Feyen DAM, McKeithan WL, Bruyneel AAN, Spiering S, Hormann L, Ulmer B, Zhang H, Briganti F, Schweizer M, Hegyi B, Liao Z, Polonen RP, Ginsburg KS, Lam CK, Serrano R, Wahlquist C, Kreymerman A, Vu M, Amatya PL, Behrens CS, Ranjbarvaziri S, Maas RGC, Greenhaw M, Bernstein D, Wu JC, Bers DM, Eschenhagen T, Metallo CM, Mercola M. Metabolic maturation media improve physiological function of human iPSC-derived cardiomyocytes. *Cell Rep* 2020;**32**:107925.
31. Dinani R, Manders E, Helmes M, Wang L, Knollmann B, Kuster DWD, van der Velden J. Real-time measurements of calcium and contractility parameters in human induced pluripotent stem cell-derived cardiomyocytes. *J Vis Exp* 2023;**195**:1–12.
32. Malan D, Friedrichs S, Fleischmann BK, Sasse P. Cardiomyocytes obtained from induced pluripotent stem cells with long-QT syndrome 3 recapitulate typical disease-specific features in vitro. *Circ Res* 2011;**109**:841–847.
33. Davis RP, Casini S, van den Berg CW, Hoekstra M, Remme CA, Dambrot C, Salvatori D, Oostwaard DW, Wilde AA, Bezzina CR, Verkerk AO, Freund C, Mummery CL. Cardiomyocytes derived from pluripotent stem cells recapitulate electrophysiological characteristics of an overlap syndrome of cardiac sodium channel disease. *Circulation* 2012;**125**:3079–3091.
34. Ma D, Wei H, Zhao Y, Lu J, Li G, Sahib NB, Tan TH, Wong KY, Shim W, Wong P, Cook SA, Liew R. Modeling type 3 long QT syndrome with cardiomyocytes derived from patient-specific induced pluripotent stem cells. *Int J Cardiol* 2013;**168**:5277–5286.
35. Berecki G, Wilders R, de Jonge B, van Ginneken AC, Verkerk AO. Re-evaluation of the action potential upstroke velocity as a measure of the Na+ current in cardiac myocytes at physiological conditions. *PLoS One* 2010;**5**:e15772.
36. Spudich JA. Three perspectives on the molecular basis of hypercontractility caused by hypertrophic cardiomyopathy mutations. *Pflugers Arch* 2019;**471**:701–717.
37. Sarkar SS, Trivedi DV, Morck MM, Adhikari AS, Pasha SN, Ruppel KM, Spudich JA. The hypertrophic cardiomyopathy mutations R403Q and R663H increase the number of myosin heads available to interact with actin. *Sci Adv* 2020;**6**:eaax0069.
38. De Stefano A, Tesauro M, Di Daniele N, Vizioli G, Schinzari F, Cardillo C. Mechanisms of SGLT2 (sodium-glucose transporter type 2) inhibition-induced relaxation in arteries from human visceral adipose tissue. *Hypertension* 2021;**77**:729–738.
39. Moellmann J, Klinkhammer BM, Droste P, Kappel B, Haj-Yehia E, Maxeiner S, Artati A, Adamski J, Boor P, Schutt K, Lopaschuk GD, Verma S, Marx N, Lehrke M. Empagliflozin improves left ventricular diastolic function of db/db mice. *Biochim Biophys Acta Mol Basis Dis* 2020;**1866**:165807.
40. Connelly KA, Zhang Y, Visram A, Advani A, Batchu SN, Desjardins JF, Thai K, Gilbert RE. Empagliflozin improves diastolic function in a nondiabetic rodent model of heart failure with preserved ejection fraction. *JACC Basic Transl Sci* 2019;**4**:27–37.
41. Pabel S, Hamdani N, Luedde M, Sossalla S. SGLT2 inhibitors and their mode of action in heart failure-has the mystery been unravelled? *Curr Heart Fail Rep* 2021;**18**:315–328.
42. Schmidt DW, Argyropoulos C, Singh N. Are the protective effects of SGLT2 inhibitors a "class-effect" or are there differences between agents? *Kidney360* 2021;**2**:881–885.
43. Suzuki Y, Kaneko H, Okada A, Itoh H, Matsuoka S, Fujiu K, Michihata N, Jo T, Takeda N, Morita H, Kamiya K, Matsunaga A, Ako J, Node K, Yasunaga H, Komuro I. Comparison of cardiovascular outcomes between SGLT2 inhibitors in diabetes mellitus. *Cardiovasc Diabetol* 2022;**21**:67.
44. Lewandowski J, Rozwadowska N, Kolanowski TJ, Malcher A, Zimna A, Rugowska A, Fiedorowicz K, Labedz W, Kubaszewski L, Chojnacka K, Bednarek-Rajewska K, Majewski P, Kurpisz M. The impact of in vitro cell culture duration on the maturation of human cardiomyocytes derived from induced pluripotent stem cells of myogenic origin. *Cell Transplant* 2018;**27**:1047–1067.
45. Ahmed RE, Anzai T, Chanthra N, Uosaki H. A brief review of current maturation methods for human induced pluripotent stem cells-derived cardiomyocytes. *Front Cell Dev Biol* 2020;**8**:178.
46. Pabel S, Reetz F, Dybkova N, Shomroni O, Salinas G, Mustroph J, Hammer KP, Hasenfuss G, Hamdani N, Maier LS, Streckfuss-Bomeke K, Sossalla S. Long-term effects of empagliflozin on excitation-contraction-coupling in human induced pluripotent stem cell cardiomyocytes. *J Mol Med (Berl)* 2020;**98**:1689–1700.
47. Ng KM, Lau YM, Dhandhania V, Cai ZJ, Lee YK, Lai WH, Tse HF, Siu CW. Empagliflozin ameliorates high glucose induced-cardiac dysfuntion in human iPSC-derived cardiomyocytes. *Sci Rep* 2018;**8**:14872.
48. Mustroph J, Wagemann O, Lucht CM, Trum M, Hammer KP, Sag CM, Lebek S, Tarnowski D, Reinders J, Perbellini F, Terracciano C, Schmid C, Schopka S, Hilker M, Zausig Y, Pabel S, Sossalla ST, Schweda F, Maier LS, Wagner S. Empagliflozin reduces ca/calmodulin-dependent kinase II activity in isolated ventricular cardiomyocytes. *ESC Heart Fail* 2018;**5**:642–648.
49. Byrne NJ, Matsumura N, Maayah ZH, Ferdaoussi M, Takahara S, Darwesh AM, Levasseur JL, Jahng JWS, Vos D, Parajuli N, El-Kadi AOS, Braam B, Young ME, Verma S, Light PE, Sweeney

G, Seubert JM, Dyck JRB. Empagliflozin blunts worsening cardiac dysfunction associated with reduced NLRP3 (nucleotide-binding domain-like receptor protein 3) inflammasome activation in heart failure. *Circ Heart Fail* 2020;**13**:e006277.
50. Chen S, Wang Q, Christodoulou A, Mylonas N, Bakker D, Nederlof R, Hollmann MW, Weber NC, Coronel R, Wakker V, Christoffels VM, Andreadou I, Zuurbier CJ. Sodium glucose cotransporter-2 inhibitor empagliflozin reduces infarct size independently of sodium glucose cotransporter-2. *Circulation* 2023;**147**:276–279.
51. Scholz W, Albus U, Counillon L, Gogelein H, Lang HJ, Linz W, Weichert A, Scholkens BA. Protective effects of HOE642, a selective sodium-hydrogen exchange subtype 1 inhibitor, on cardiac ischaemia and reperfusion. *Cardiovasc Res* 1995;**29**:260–268.
52. Chung YJ, Park KC, Tokar S, Eykyn TR, Fuller W, Pavlovic D, Swietach P, Shattock MJ. Off-target effects of sodium-glucose co-transporter 2 blockers: empagliflozin does not inhibit Na+/H+ exchanger-1 or lower [Na+]i in the heart. *Cardiovasc Res* 2021;**117**:2794–2806.
53. Zuurbier CJ, Baartscheer A, Schumacher CA, Fiolet JWT, Coronel R. Sodium-glucose co-transporter 2 inhibitor empagliflozin inhibits the cardiac Na+/H+ exchanger 1: persistent inhibition under various experimental conditions. *Cardiovasc Res* 2021;**117**:2699–2701.
54. Chung YJ, Park KC, Tokar S, Eykyn TR, Fuller W, Pavlovic D, Swietach P, Shattock MJ. SGLT2 inhibitors and the cardiac Na+/H+ exchanger-1: the plot thickens. *Cardiovasc Res* 2021;**117**:2702–2704.
55. Uthman L, Nederlof R, Eerbeek O, Baartscheer A, Schumacher C, Buchholtz N, Hollmann MW, Coronel R, Weber NC, Zuurbier CJ. Delayed ischaemic contracture onset by empagliflozin associates with NHE1 inhibition and is dependent on insulin in isolated mouse hearts. *Cardiovasc Res* 2019;**115**:1533–1545.
56. Arjun S, Bell RM. SGLT2 inhibitors: reviving the sodium-hydrogen exchanger cardioprotection hypothesis? *Cardiovasc Res* 2019;**115**:1454–1456.
57. Olivotto I, Camici PG, Merlini PA, Rapezzi C, Patten M, Climent V, Sinagra G, Tomberli B, Marin F, Ehlermann P, Maier LS, Fornaro A, Jacobshagen C, Ganau A, Moretti L, Hernandez Madrid A, Coppini R, Reggiardo G, Poggesi C, Fattirolli F, Belardinelli L, Gensini G, Mugelli A. Efficacy of ranolazine in patients with symptomatic hypertrophic cardiomyopathy: the RESTYLE-HCM randomized, double-blind, placebo-controlled study. *Circ Heart Fail* 2018;**11**:e004124.
58. Juni RP, Kuster DWD, Goebel M, Helmes M, Musters RJP, van der Velden J, Koolwijk P, Paulus WJ, van Hinsbergh VWM. Cardiac microvascular endothelial enhancement of cardiomyocyte function is impaired by inflammation and restored by empagliflozin. *JACC Basic Transl Sci* 2019;**4**:575–591.
59. Han L, Li Y, Tchao J, Kaplan AD, Lin B, Li Y, Mich-Basso J, Lis A, Hassan N, London B, Bett GC, Tobita K, Rasmusson RL, Yang L. Study familial hypertrophic cardiomyopathy using patient-specific induced pluripotent stem cells. *Cardiovasc Res* 2014;**104**:258–269.
60. Prondzynski M, Lemoine MD, Zech AT, Horvath A, Di Mauro V, Koivumaki JT, Kresin N, Busch J, Krause T, Kramer E, Schlossarek S, Spohn M, Friedrich FW, Munch J, Laufer SD, Redwood C, Volk AE, Hansen A, Mearini G, Catalucci D, Meyer C, Christ T, Patten M, Eschenhagen T, Carrier L. Disease modeling of a mutation in alpha-actinin 2 guides clinical therapy in hypertrophic cardiomyopathy. *EMBO Mol Med* 2019;**11**:e11115.
61. Westermann D, Knollmann BC, Steendijk P, Rutschow S, Riad A, Pauschinger M, Potter JD, Schultheiss HP, Tschope C. Diltiazem treatment prevents diastolic heart failure in mice with familial hypertrophic cardiomyopathy. *Eur J Heart Fail* 2006;**8**:115–121.
62. Wu H, Yang H, Rhee JW, Zhang JZ, Lam CK, Sallam K, Chang ACY, Ma N, Lee J, Zhang H, Blau HM, Bers DM, Wu JC. Modelling diastolic dysfunction in induced pluripotent stem cell-derived cardiomyocytes from hypertrophic cardiomyopathy patients. *Eur Heart J* 2019;**40**:3685–3695.
63. Durak A, Olgar Y, Degirmenci S, Akkus E, Tuncay E, Turan B. A SGLT2 inhibitor dapagliflozin suppresses prolonged ventricular-repolarization through augmentation of mitochondrial function in insulin-resistant metabolic syndrome rats. *Cardiovasc Diabetol* 2018;**17**:144.
64. Hirt MN, Boeddinghaus J, Mitchell A, Schaaf S, Börnchen C, Müller C, Schulz H, Hubner N, Stenzig J, Stoehr A, Neuber C, Eder A, Luther PK, Hansen A, Eschenhagen T. Functional improvement and maturation of rat and human engineered heart tissue by chronic electrical stimulation. *J Mol Cell Cardiol* 2014;**74**:151–161.
65. Cui C, Geng L, Shi J, Zhu Y, Yang G, Wang Z, Wang J, Chen M. Structural and electrophysiological dysfunctions due to increased endoplasmic reticulum stress in a long-term pacing model using human induced pluripotent stem cell-derived ventricular cardiomyocytes. *Stem Cell Res Ther* 2017;**8**:109.
66. Begley CG, Ioannidis JP. Reproducibility in science: improving the standard for basic and preclinical research. *Circ Res* 2015;**116**:116–126.
67. Horváth A, Lemoine MD, Löser A, Mannhardt I, Flenner F, Uzun AU, Neuber C, Breckwoldt K, Hansen A, Girdauskas E, Reichenspurner H, Willems S, Jost N, Wettwer E, Eschenhagen T, Christ T. Low resting membrane potential and low inward rectifier potassium currents are not inherent features of hiPSC-derived cardiomyocytes. *Stem Cell Reports* 2018;**10**:822–833.
68. Uzun AU, Mannhardt I, Breckwoldt K, Horváth A, Johannsen SS, Hansen A, Eschenhagen T, Christ T. Ca(2+)-currents in human induced pluripotent stem cell-derived cardiomyocytes effects of two different culture conditions. *Front Pharmacol* 2016;**7**:300.
69. Lemoine MD, Mannhardt I, Breckwoldt K, Prondzynski M, Flenner F, Ulmer B, Hirt MN, Neuber C, Horváth A, Kloth B, Reichenspurner H, Willems S, Hansen A, Eschenhagen T, Christ T. Human iPSC-derived cardiomyocytes cultured in 3D engineered heart tissue show physiological upstroke velocity and sodium current density. *Sci Rep* 2017;**7**:5464.
70. Iqbal Z, Ismaili D, Dolce B, Petersen J, Reichenspurner H, Hansen A, Kirchhof P, Eschenhagen T, Nikolaev VO, Molina CE, Christ T. Regulation of basal and norepinephrine-induced cAMP and I_{Ca} in hiPSC-cardiomyocytes: effects of culture conditions and comparison to adult human atrial cardiomyocytes. *Cell Signal* 2021;**82**:109970.